5-2024

CAELUS: Cubesat Array for the ExpLoration of the Uranus System

Dylan George Heidenrich Barnes
Florida Institute of Technology, dbarnes2018@my.fit.edu

CAELUS: Cubesat Array for the ExpLoration of the Uranus System

by

Dylan George Heidenrich Barnes

Bachelor of Science
Aerospace Engineering
Florida Institute of Technology
2022

A thesis
submitted to the College of Engineering and Science
at Florida Institute of Technology
in partial fulfillment of the requirements
for the degree of

Master of Science
in
Aerospace Engineering

Melbourne, Florida
May, 2024

We the undersigned committee
hereby approve the attached thesis

CAELUS: Cubesat Array for the ExpLoration of the Uranus System

by

Dylan George Heidenrich Barnes

Paula do Vale Pereira, Ph.D.
Assistant Professor
Aerospace, Physics, and Space Sciences
Major Advisor

Eric D. Swenson, Ph.D.
Associate Professor
Aerospace, Physics, and Space Sciences

Ryan T. White, Ph.D.
Assistant Professor
Mathematics and Systems Engineering

Ratneshwar Jha, Ph.D.
Professor and Department Head
Aerospace, Physics, and Space Sciences

Abstract

Title:

CAELUS: Cubesat Array for the ExpLoration of the Uranus System

Author:

Dylan George Heidenrich Barnes

Major Advisor:

Paula do Vale Pereira, Ph.D.

Following recommendations from the 2023-2032 Planetary Science and Astrobiology Decadal Survey [59], we propose a novel Pre-Phase A level Uranus exploration mission concept that is centered on using swarms of small spacecraft to observe the Uranus system. This mission could act as a supplement to the Flagship Uranus Orbiter and Probe mission detailed in said Decadal Survey [74]. We propose launching a 4,500 kg spacecraft on an Earth-Jupiter-Uranus gravity assist transfer trajectory with a transfer time of six years, launching in 2033 and arriving at Uranus in 2039. This shorter transfer time and accelerated development timeline would allow for an earlier arrival date than a traditional flagship spacecraft. Arriving by 2039 would make it possible to observe the changing of the Uranian seasons from solstice to equinox, helping us better understand the atmospheric dynamics, as well as take advantage of a unique planetary alignment for an efficient interplanetary transfer. To maintain the quality of data collection while minimizing mass, we propose that the spacecraft be composed

of a carrier spacecraft with a 3,848 kg wet mass, which would be used primarily for communications and orbital transfers, and a swarm of CubeSats with a combined wet mass of 640 kg, which would house the instrumentation. The swarm of 16 CubeSats of approximately 40 kg each would be divided into 4 groups of 4 identical spacecraft. Each group will be equipped with specialized instrumentation, exploring Uranus more extensively and performing planned plunges into its atmosphere. This spatial distribution of the instrumentation would allow for measurements that require multiple perspectives of observation, such as radio occultation and precision gravity measurements. The results shown in this Thesis demonstrate that a high level analysis of such a deep space small satellite mission converges to a viable solution.

Table of Contents

List of Figures

List of Tables

List of Symbols, Nomenclature or Abbreviations

PSADS	Planetary Science and Astrobiology Decadal Survey
UOP	Uranus Orbiter and Probe
LEO	Low Earth Orbit
ESA	European Space Agency
MMS	Magnetospheric Multiscale mission
EJU	Earth - Jupiter - Uranus
EJ	Earth - Jupiter
SLS	Space Launch System
C3	Characteristic Energy
RJ	Radius of Jupiter
RU	Radius of Uranus
SSB	Solar System Barycenter
ConOps	Concept of Operations
tSTM	Truncated Science Traceability Matrix
CAD	Computer Aided Design
COTS	Commercial Off The Shelf
ADCS	Attitude Determination and Control System
Comms	Communications
IMU	Inertial Mass Unit
SOH	State of Health
RTG	Radioisotope Thermoelectric Generators
MMRTG	Multi-Mission Radioisotope Thermoelectric Generators
TRC	thermoradiative cell
GPHS	General Purpose Heat Sources
RHU	Radioisotope Heater Units
DSN	Deep Space Network
P-POD	Poly Picosatellite Orbital Deployer
BOL	Beginning of Life
EoM	End of Mission

Acknowledgements

I would like to thank my advisor, Dr. do Vale Pereira, for her support and enthusiasm along the journey that was this project. I would also like to thank my committee members, Dr. White and Dr. Swenson, for their suggestions, time, and expertise. Finally, I would like to thank Florida Tech's Department of Aerospace, Physics, and Space Sciences, Department of Residence Life, and Florida Institute of Technology as a whole for their financial support and providing a place to grow all these years.

Dedication

To my family, for their unceasing support. May we travel ever upwards.

Chapter 1

Introduction

1.1 The Case for a Mission to Uranus

The ice giant Uranus remains one of the least explored major celestial bodies in our solar system. Despite eleven probes launched to study the major bodies of the outer solar system as of the launch of JUICE in 2023, only Voyager 2 has ever studied either of the ice giants, performing a flyby of Uranus in 1986 and Neptune in 1989 [12].

In 2022, the National Academies of Sciences, Engineering, and Medicine recommended a return to Uranus with the Uranus Orbiter and Probe (UOP), prioritizing it as their highest-priority Flagship mission in the 2023-2032 "Origins, Worlds, and Life" Planetary Science and Astrobiology Decadal Survey (PSADS) [59]. The UOP would deliver an in-situ probe to the Uranian atmosphere and conduct a multi-year orbital tour to answer questions about Uranus's origin, interior, atmosphere, magnetosphere, satellites, and rings.

First discussed in the previous decadal survey [60], the proposed UOP is a 7,200 kg spacecraft comprised of an orbiter and an in-situ probe, similar to the Huygens probe and the Cassini spacecraft [54]. The current PSADS and supporting documentation

suggests that the UOP be launched in the early 2030s with a 13-year transfer time along an Earth-Earth-Jupiter-Uranus trajectory and a 4.5-year science mission phase, leading to an arrival around 2044 and mission operations through 2049 [74]. However, such a timeline appears increasingly unlikely as the optimal launch dates are fewer than eight years away as of the writing of this document, and Flagship missions normally typically require more than ten year development timelines, not taking delays into account [13].

However, there are alternative mission possibilities that would still allow the launch of a spacecraft within the eight year goal. If the payload mass is reduced, a more powerful launch vehicle is used, or both, alternate trajectories become possible. History supports these kinds of trajectories, as Voyager 2 reached Uranus 8 years after launch [83], and New Horizons passed Uranus's orbit just over 5 years after launch [31, 8]. An accelerated transfer with fewer flybys also requires fewer maneuvers and therefore reduces mission complexity, and therefore risk.

There are also significant scientific benefits to arriving at Uranus sooner. Because of its unique axial tilt of approximately 98°, Uranus has an uncommonly long seasonal pattern, taking 84 years to complete one full cycle from winter solstice to summer solstice and back to the winter solstice [81]. From approximately 2020 until approximately 2040, the northern hemisphere will be facing sunlight while the southern hemisphere will be in darkness [33] leading into an equinox in 2049 [35]. Arriving around 2040 would allow the spacecraft to be present for the change from solstice to equinox, allowing it to observe the transition between seasons and providing unique insights that may be lost if the spacecraft were to arrive after the transition had already taken place. Thus, as a UOP Flagship mission arrival at or before the upcoming transition to the solstice becomes unlikely, the possibility arises for a lower-budget mission conducted in parallel with the Flagship that could launch in the early 2030s and support it by

collecting data ahead of the arrival of the UOP.

This new mission concept, developed with the goal of answering as many questions from the PSADS as possible, would be able to supplement and expand upon the data collected by the initially proposed 7,200 kg spacecraft. Of the twelve thematic questions posed by the most recent PSADS, UOP seeks to at least partially address eleven of them, answering questions about origins, processes, habitability, and interconnection [74]. Of particular interest are the questions about how ice giants like Uranus form, what external factors are altering the planet, satellites, and ring compositions, and what interior structure produces Uranus's complex magnetosphere. To answer as many questions as possible while maintaining a significantly lesser mass, we propose a swarm of CubeSats be flown to Uranus at an accelerated timeline, and thus having multiple lighter, less expensive eyes on the Uranian system before it enters into equinox while taking advantage of the unique benefits that CubeSats offer.

1.2 CubeSats Around and Beyond Earth

1.2.1 CubeSats in LEO

Since the first CubeSat was launched in 2003, they have been used as a fast, inexpensive method to perform a task in orbit. CubeSats have been used for a variety of purposes, including technology demonstrations, communications, education, and viable science generation [76]. This science takes many forms, including heliophysics, astrophysics, lunar science, and most commonly, Earth science through planetary observation [19].

The use of CubeSats for planetary observation is well documented. Examples include the LEMUR constellation [3], CanX-2 [70], QuakeSat-1 [43], and the TROPICS constellation [17], whose missions involved Earth observation on demand, atmospheric spectroscopy, magnetosphere fluctuations, and microwave spectroscopy, respectively

[19, 73].

Additionally, it is important to note that two of the previous four examples used multiple CubeSats in formation flight, called a 'swarm' or 'constellation'. Using CubeSats in this way allows for significant benefits over single spacecraft, including interoperability, higher data capture, bandwidth redundancy, rich power budget, reduced mission failure rates, and the ability to obtain global coverage and measurements [62, 67, 10]. Especially of interest is the ability of a CubeSat swarm to reconstruct three-dimensional models of observed phenomena through observing it from multiple viewpoints, an ability that has been demonstrated to be accurate within 10s of meters [7].

There have been several successful demonstrations of formation flight among several spacecraft in the past [21]. An additional example to those above is the GRACE mission, which used two spacecraft to perform precise measurements of the gravitational potential of the Earth and its variations around the globe [36]. Other examples are the DICE mission, which used two CubeSats in formation to measure ionospheric plasma density and magnetic fields [27], the AeroCube-4 mission, which was composed of three CubeSats and demonstrated changes in orbital position between the satellites [28], ESA's Cluster II mission, which uses four spacecraft in formation to study Earth's magnetic field [26], and the Magnetospheric Multiscale mission (MMS), which also studies Earth's magnetic field and its interactions with the Sun [18].

That is not to say, however, that CubeSats do not have their own unique challenges when compared to traditional, larger spacecraft. While generally less expensive and faster to launch due to reduced mass, volume, power requirements, and part standardization, they also have a reduced mission timeline, rarely functioning for longer than one or two years [61]. In the case of most LEO CubeSats, this is due to orbit decay from atmospheric drag [44], and early failure (primarily in university-led CubeSats).

Additionally, although reduced mass, volume, and power requirements typically mean a decrease in cost, they also constrain payloads, requiring smaller and less power intensive instruments, which generally also reduces the instruments capacity, versatility, or both.

CubeSats also tend to have long range communication restrictions. Because of both the power budget and the small size factor, both of the standard methods of improving communication fidelity, increasing antenna size and increasing transmission power, are difficult. CubeSats in LEO generally do not have to deal with this issue, as they are close enough to a ground station that the limitations of the form factor can be mitigated [69], but this is a major design challenge for any CubeSat in a higher orbit, or beyond Earth's sphere of influence entirely [32].

1.2.2 Interplanetary CubeSats

While most CubeSats have been launched into LEO for Earth observation tasks, we are not the first to propose using them beyond the Earth. CubeSats have been launched into orbits or rendezvous with bodies other than Earth several times, all greatly successful. LICIACube was launched along with the DART mission to observe the DART spacecraft's impact with the asteroid Dymorphos [79, 24]. CAPSTONE and Lunar Flashlight were both sent to the Moon as pathfinder and technology demonstration missions, respectively [29, 37]. Finally, the twin MarCO CubeSats were sent to Mars to both support the Mars InSight landing and as technology demonstrations, being the first CubeSats sent on an interplanetary mission [71].

Continuing the momentum of CubeSats being used in interplanetary space and taking into account the PSADS for this decade, we propose a CubeSat mission to Uranus. This mission would act in support of the traditional, single spacecraft UOP Flagship mission to Uranus by collecting data that the Flagship is not able to. By

sending a lighter, less expensive spacecraft on a 6-year Earth-Jupiter-Uranus (EJU) trajectory, it is possible to arrive seven years earlier than a traditional flagship mission launched at the same time, thus arriving in the Uranus system in time to observe the transition of the planet from solstice to equinox and utilizing the advantageous planetary positioning that occurs in the early 2030s. By sending CubeSats instead of a single spacecraft, we are able to take advantage of the unique methods of data collection only available to CubeSats, therefore occupying a separate scientific "niche."

1.3 Thesis Overview

In this thesis, we will develop a Pre-Phase A level mission concept design for a CubeSat swarm mission to Uranus, with the layout detailed below.

Chapter 1 has explained the background of the mission and conducted a review of previous similar missions.

Chapter 2 will cover the overarching mission planning and interplanetary trajectory analysis. It includes the mission definition, statement, and objectives, a concept of operations, a science traceability matrix, and the proposed interplanetary trajectory.

Chapter 3 will discuss spacecraft design. It is broken into two major sections, CubeSat Design and Carrier Spacecraft Design. Each major section is further broken down into spacecraft subsystems.

Chapter 4 will conclude this thesis with a summary and future steps.

Chapter 2

Mission Definition

We propose sending a swarm of CubeSats to Uranus contained within a carrier spacecraft. The CubeSats would be primarily responsible for data gathering, while the carrier would be used for transportation while traveling to Uranus and then as a communications hub once in orbit, taking advantage of its larger size and power budget to act as a relay between the CubeSats and the Earth.

There are two primary advantages to using CubeSats to gather data when compared to a larger, traditional spacecraft. One advantage is due to the nature of a CubeSat swarm: a swarm is a distributed system, and so it is possible to perform data collection in ways that would otherwise be impossible, such as observing the same phenomena from different angles to reconstruct a 3D representation, measuring the fluctuations in gravity around Uranus through a radio link between two different spacecraft in the same orbit, performing radio occultation measurements to determine atmospheric composition, or studying plasma and magnetic field phenomena as seen with Cluster II or MMS [26, 18]. A distributed network also provides additional redundancy and interoperability when compared to a single spacecraft.

The second primary advantage to using CubeSats as data collection devices is their

ability to specialize. Any individual CubeSat is able to be specialized around a specific instrument to a much greater degree than a multipurpose spacecraft would, allowing for more specialized operation and more focused and streamlined data collection.

2.1 Mission Statement and Objectives

This mission aims to gather data on the composition, interior, atmosphere, and magnetosphere of Uranus, investigate its rings, and study its moons and their evolution throughout time. From this mission statement, five science objectives and one technology demonstration objective are formed.

1. *Science Objective 1:* Measure the internal composition of Uranus.
2. *Science Objective 2:* Measure the atmospheric structure, dynamics, climate, circulation, and meteorological patterns of Uranus.
3. *Science Objective 3:* Measure the composition and structure of the Uranian moons and rings and discover their geological history.
4. *Science Objective 4:* Measure the structure dynamics, and ion composition of Uranus's magnetosphere and ionosphere.
5. *Science Objective 5:* Determine how Uranus interacts with its environment, moons, and rings.
6. *Technology Demonstration Objective:* Demonstrate that a swarm of CubeSats can perform missions meaningful to the scientific community.

If these science objectives are achieved, this mission will at least partially answer multiple questions from the PSADS, including significant sections of thematic questions

1, 2, 4, 5, 7, 8, 10, and 11 [59]. Furthermore, the method by which a swarm of spacecraft could answer these questions is different from that of a single traditional spacecraft, and would therefore be supplemental to a flagship UOP spacecraft.

2.2 Interplanetary Trajectory

The interplanetary transfer trajectory proposed is a 6-year Earth-Jupiter-Uranus (EJU) cruise, relying heavily on the excess energy of the launch vehicle, as said vehicle is the only source of the Earth exit velocity. The most powerful currently commercially available option is to use a Falcon Heavy Expendable Launcher, which is able to launch 63,800 kg to LEO [1]. Using this 6-year trajectory with a Falcon Heavy Expendable Launcher would allow for the delivered spacecraft to have a wet mass of around 1600 kg at launch. While this is substantial, it is not enough for this mission design, as a wet mass of at least 3000 kg is desired. Therefore, we must look into launch vehicles that are projected to be active in the early 2030s, which includes both the SpaceX Starship and the Space Launch System (SLS) [2, 30].

The required ΔVs for trajectory analysis were calculated using numerical solutions to Lambert's problem [41] and planetary ephemeris data from the NASA/Caltech Jet Propulsion Laboratory's Horizons database [39]. The code written for this thesis starts by taking the launch date, flyby date, and arrival date to calculate how much energy the launch vehicle would need to deliver to the spacecraft to put it on the correct hyperbolic Earth exit trajectory that to result on the desired flyby and arrival dates. Heavier spacecraft require more energy from the rocket, so a common way of comparing rockets is to look at how much energy is delivered per unit of mass of the spacecraft (the characteristic energy), typically in J/kg or km^2/s^2 and commonly called "C3". The code written for this thesis then uses the C3 curve of multiple launch vehicles and

the performance characteristics of the spacecraft's thruster to optimize a trajectory so that we could have the heaviest possible spacecraft dry mass launched in the desired trajectory. The payload mass to C3 curves can be seen in Figure 2.1 with values used in Table 2.1. Payload mass-to-orbit curves are not publicly available for Starship, so values were approximated based on Falcon Heavy characteristics and comparative lift to LEO. The trajectory simulation code is included in Appendix A.

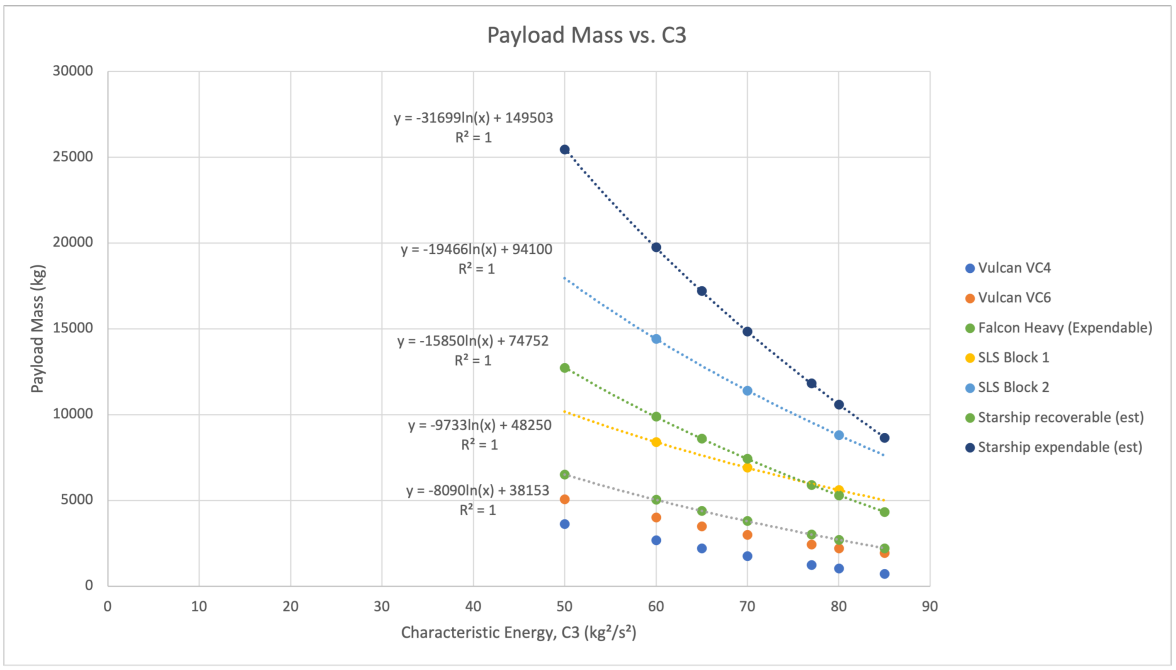

Figure 2.1: Launch Mass vs. C3 for a selection of launch vehicles

For this analysis we used the SLS Block 2 as our launch vehicle and a SpaceX Merlin 1D Vacuum engine [50] as the spacecraft thruster. The results are indexed by year and by *tm*, a variable used in solving Lambert's problem. If *tm* is 1 the portion of the solution ellipse travelled by the spacecraft will be between 0° and 180°, while if *tm* is -1 the solution will be between 180° and 360°. Results of simulation and a visualized trajectory can be seen in Figures 2.3-2.12. The trajectory simulation showed that the optimal interplanetary transfer between Earth and Uranus that launches in the early 2030s launches on May 5th, 2033, flies by Jupiter for a gravity assist maneuver

C3 (kg^2/s^2)	Payload Mass (kg)			
	Vulcan VC4	Vulcan VC6	Falcon Heavy Exp.	SLS Block 1
60	2669	3997	5043	8400
70	1747	2977	3788	6900
80	1021	2189	2700	5600
C3 (kg^2/s^2)	Payload Mass (kg)			
	SLS Block 2	Starship Rec. (est)	Starship Exp. (est)	
60	14400	9880	19760	
70	11400	7422	14845	
80	8800	5290	10579	

Table 2.1: Launch Mass vs. C3 for a selection of launch vehicles. Used to create Figure 2.1. [75, 66].

on October 1st, 2034, and arrives at the Uranus system on March 18th, 2039. This trajectory allows for a spacecraft wet mass of 4488 kg and a dry mass of 3344 kg, giving the best balance between mass and travel time. The optimal solution described is Figure 2.11. and a simplified summary of the transfer can be seen in Figure 2.2 along with a transfer thrust timeline.

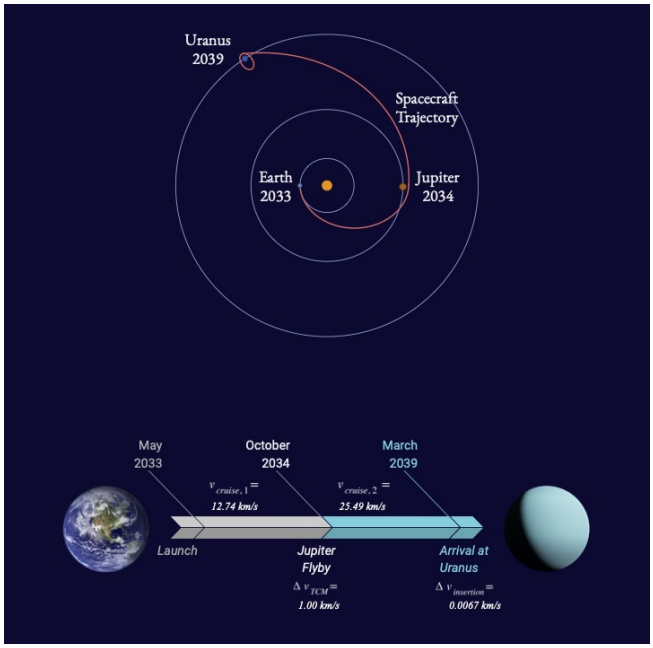

Figure 2.2: Simplified Trajectory Summary. Corresponds to Figure 2.11. ΔV_{TCM} is the ΔV required for the trajectory correction burn for the gravity assist. $\Delta V_{insertion}$ is the Δ V required to enter the capture orbit around Uranus. Image not to scale.

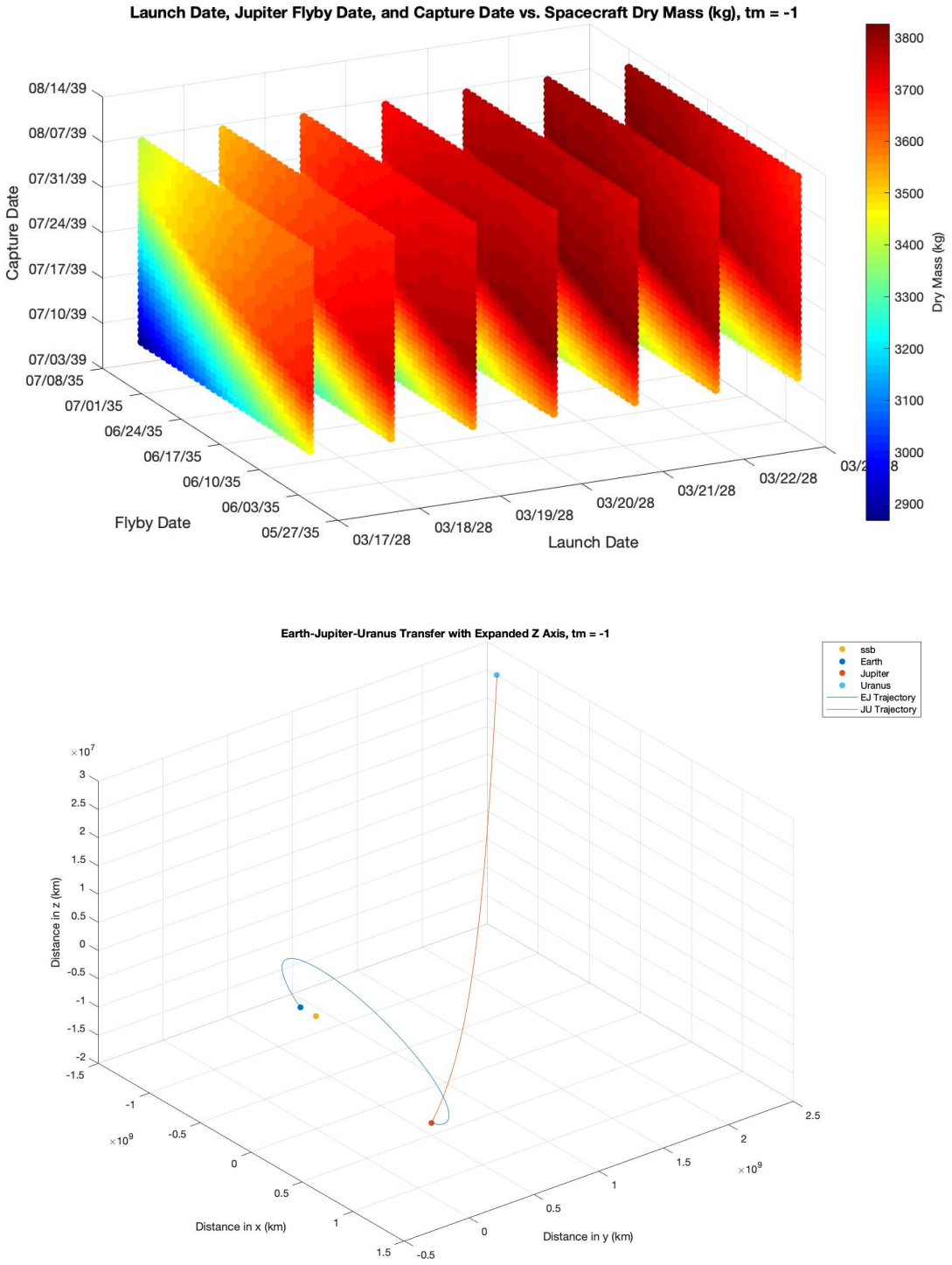

Figure 2.3: Trajectory simulation results for 2028, *tm* -1.

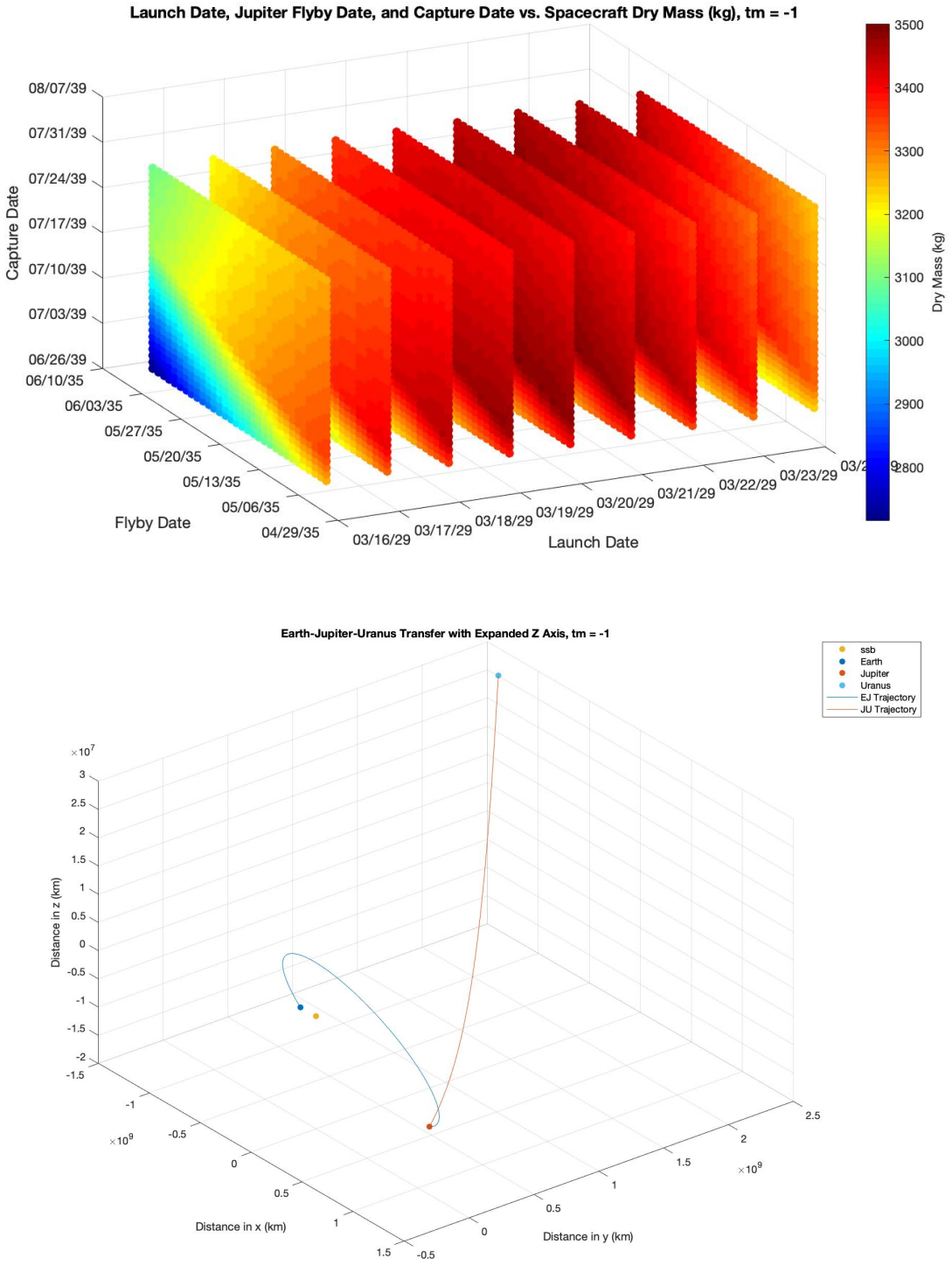

Figure 2.4: Trajectory simulation results for 2029, *tm* -1.

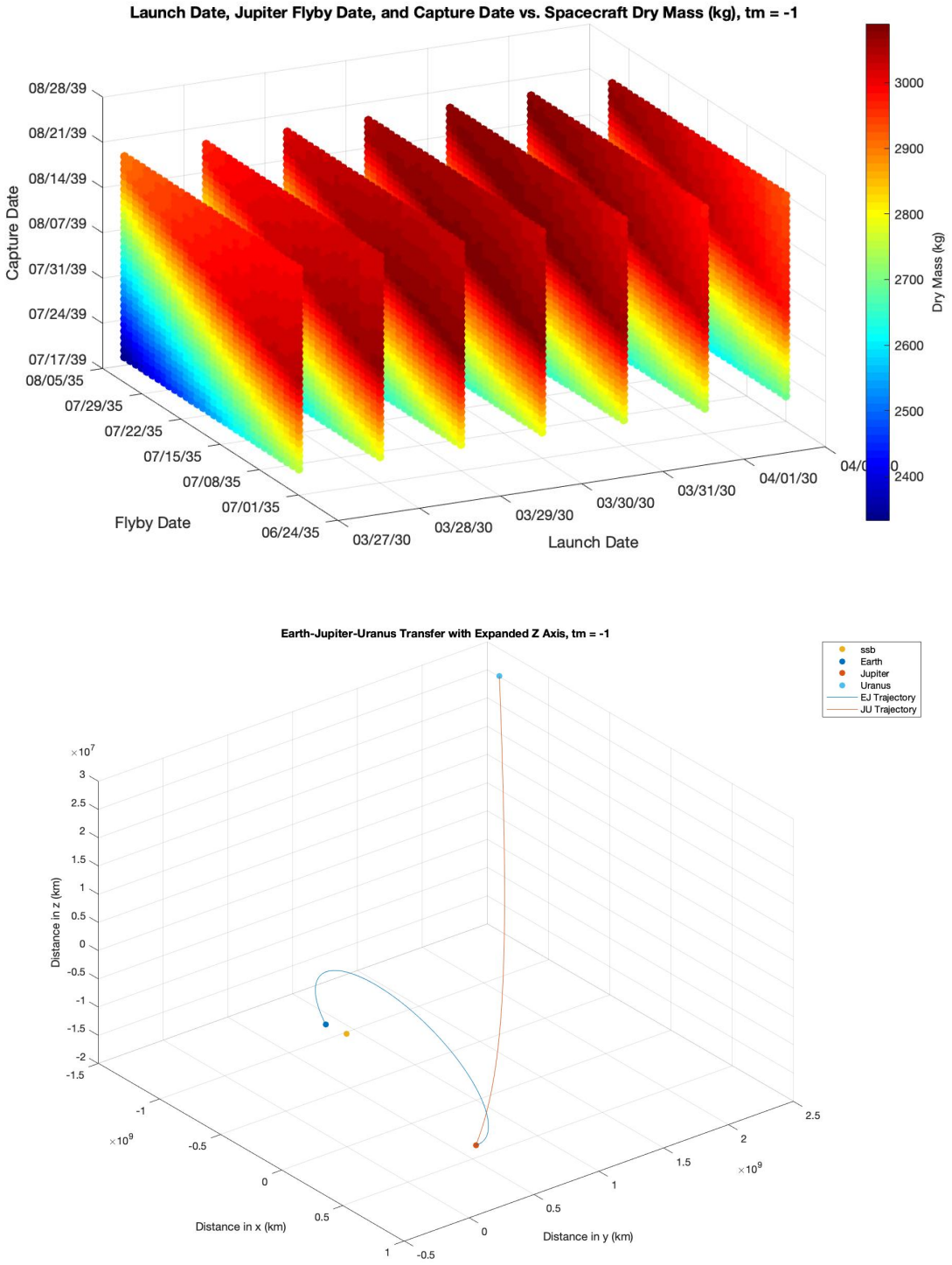

Figure 2.5: Trajectory simulation results for 2030, *tm* -1.

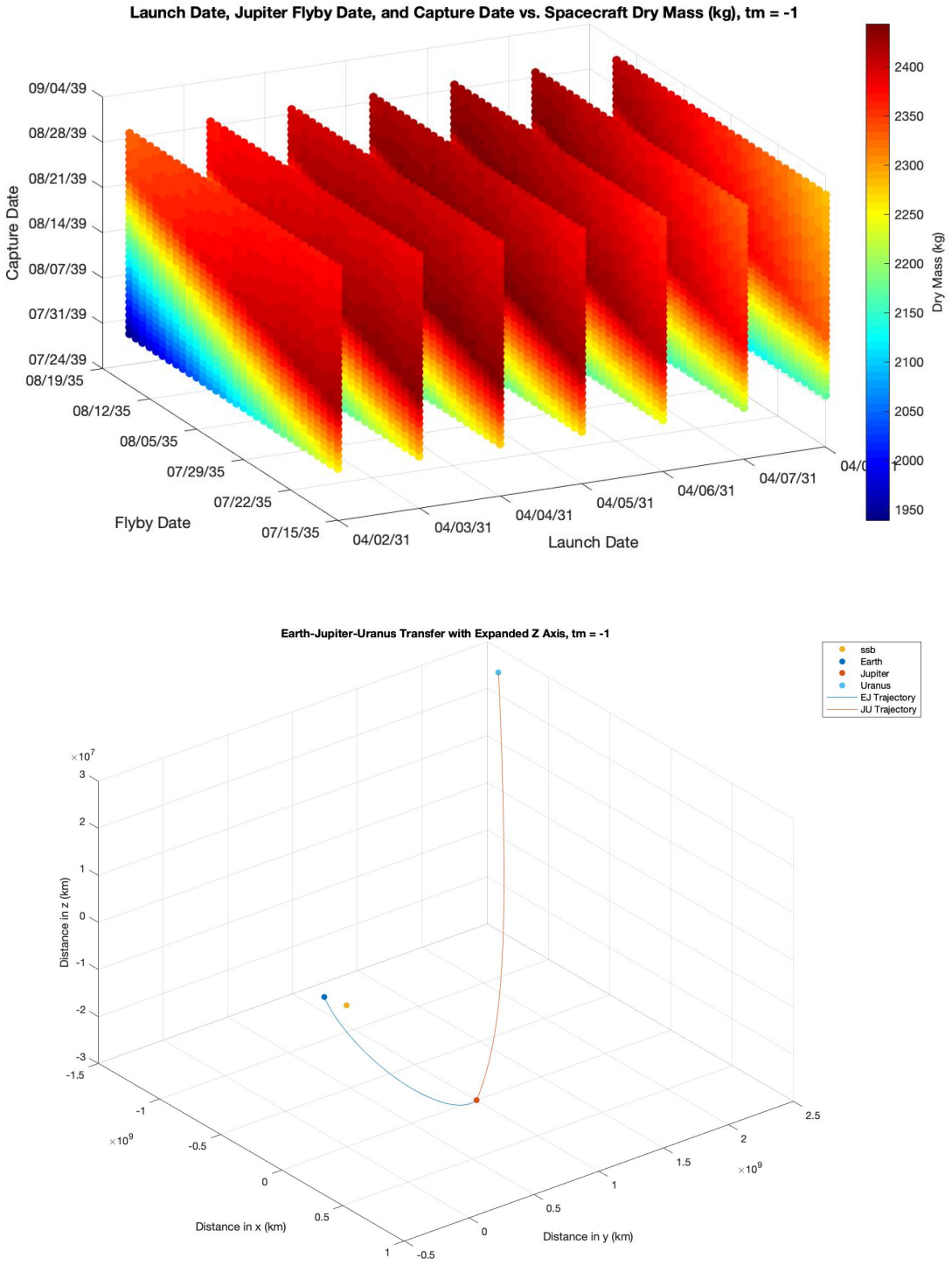

Figure 2.6: Trajectory simulation results for 2031, *tm* -1.

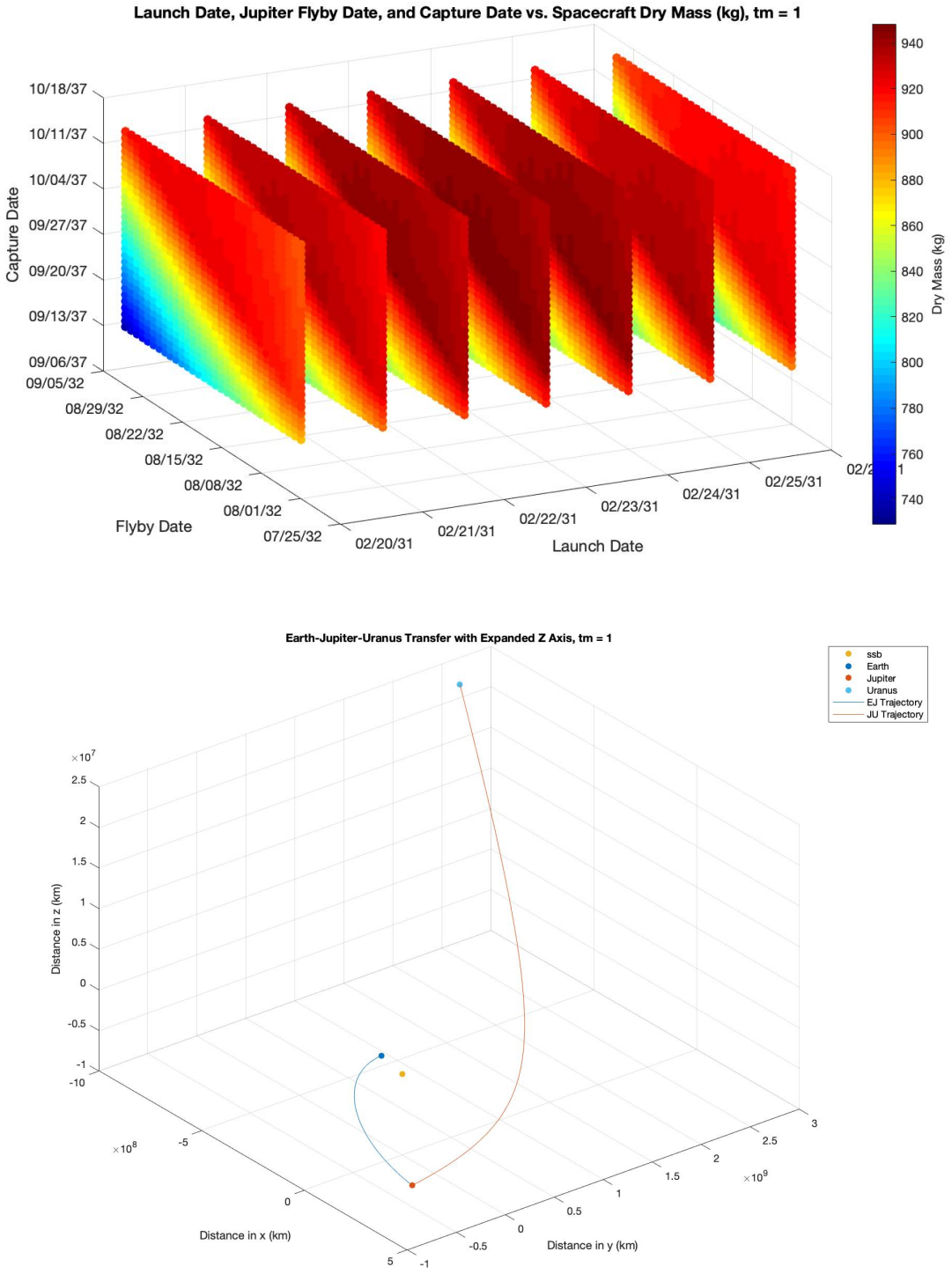

Figure 2.7: Trajectory simulation results for 2031, *tm* 1.

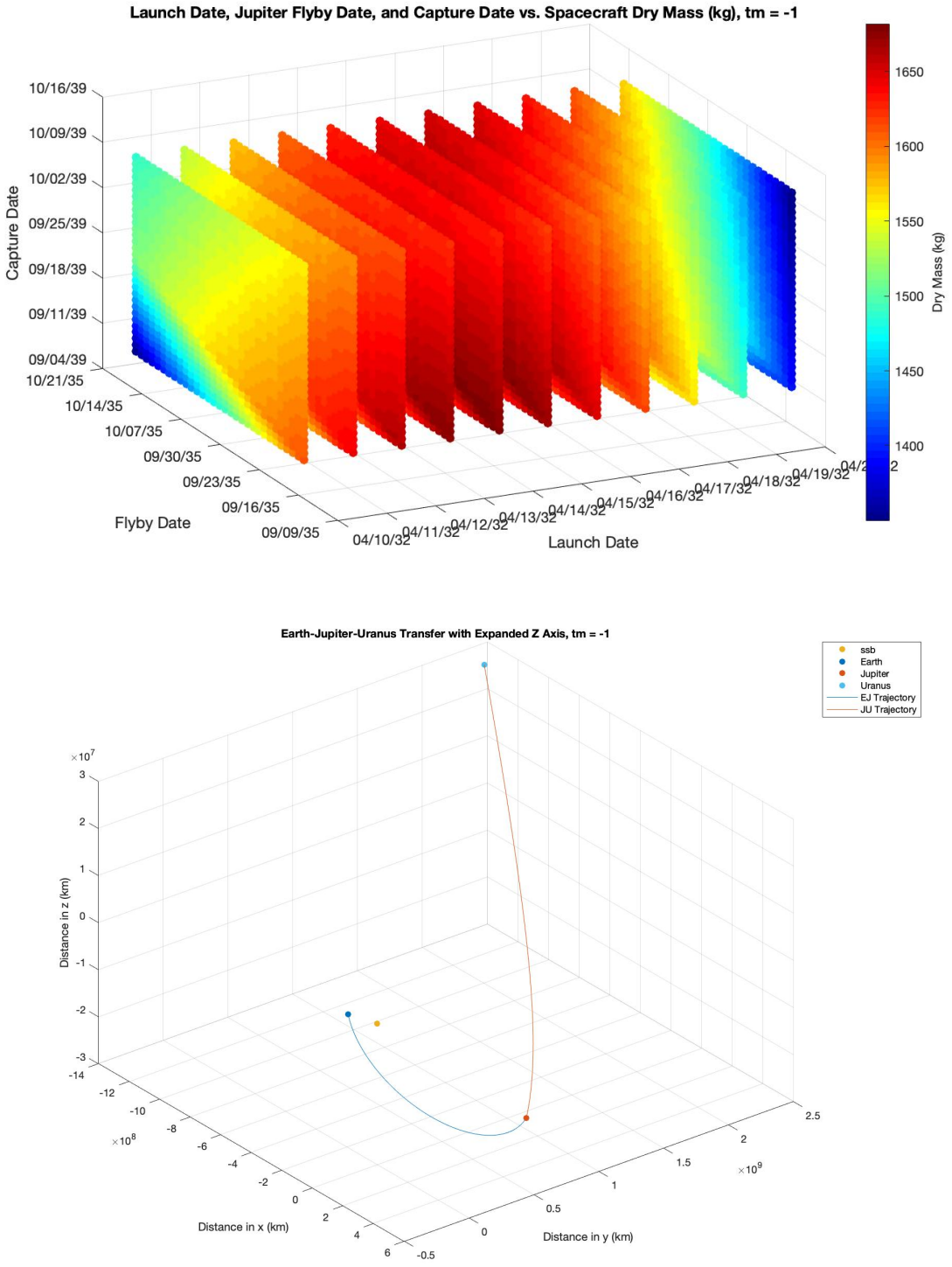

Figure 2.8: Trajectory simulation results for 2032, *tm* -1.

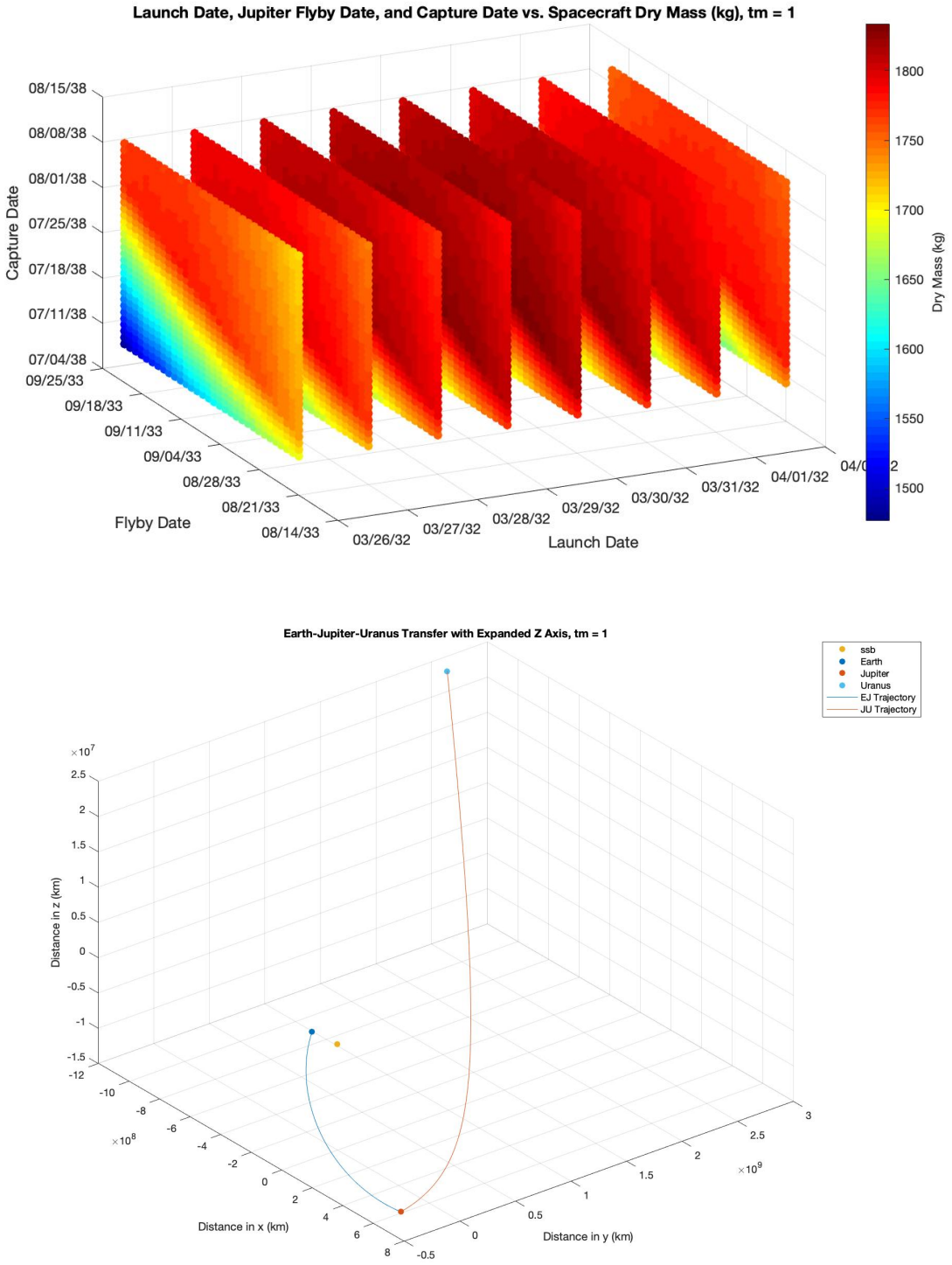

Figure 2.9: Trajectory simulation results for 2032, *tm* 1.

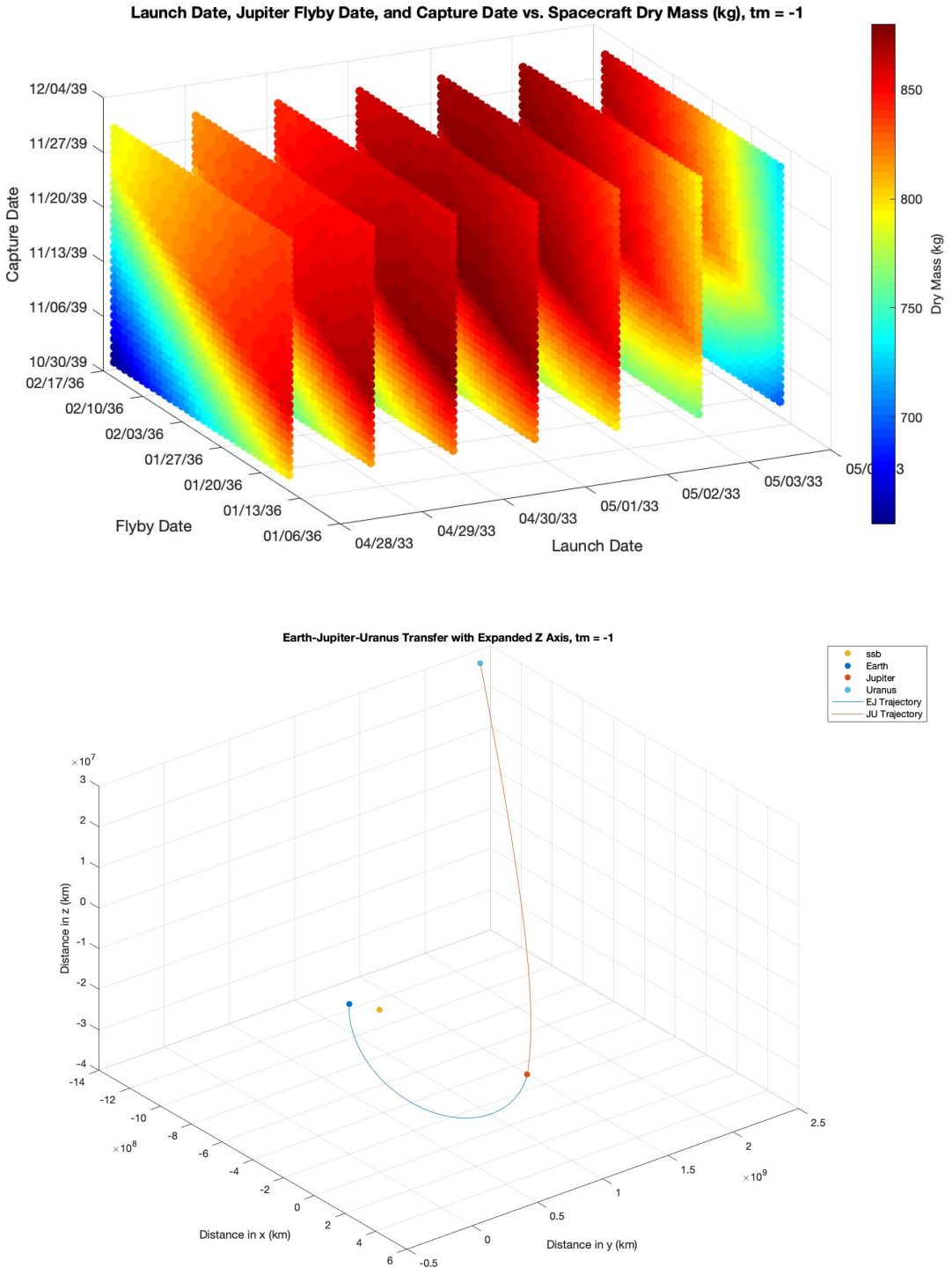

Figure 2.10: Trajectory simulation results for 2033, *tm* -1.

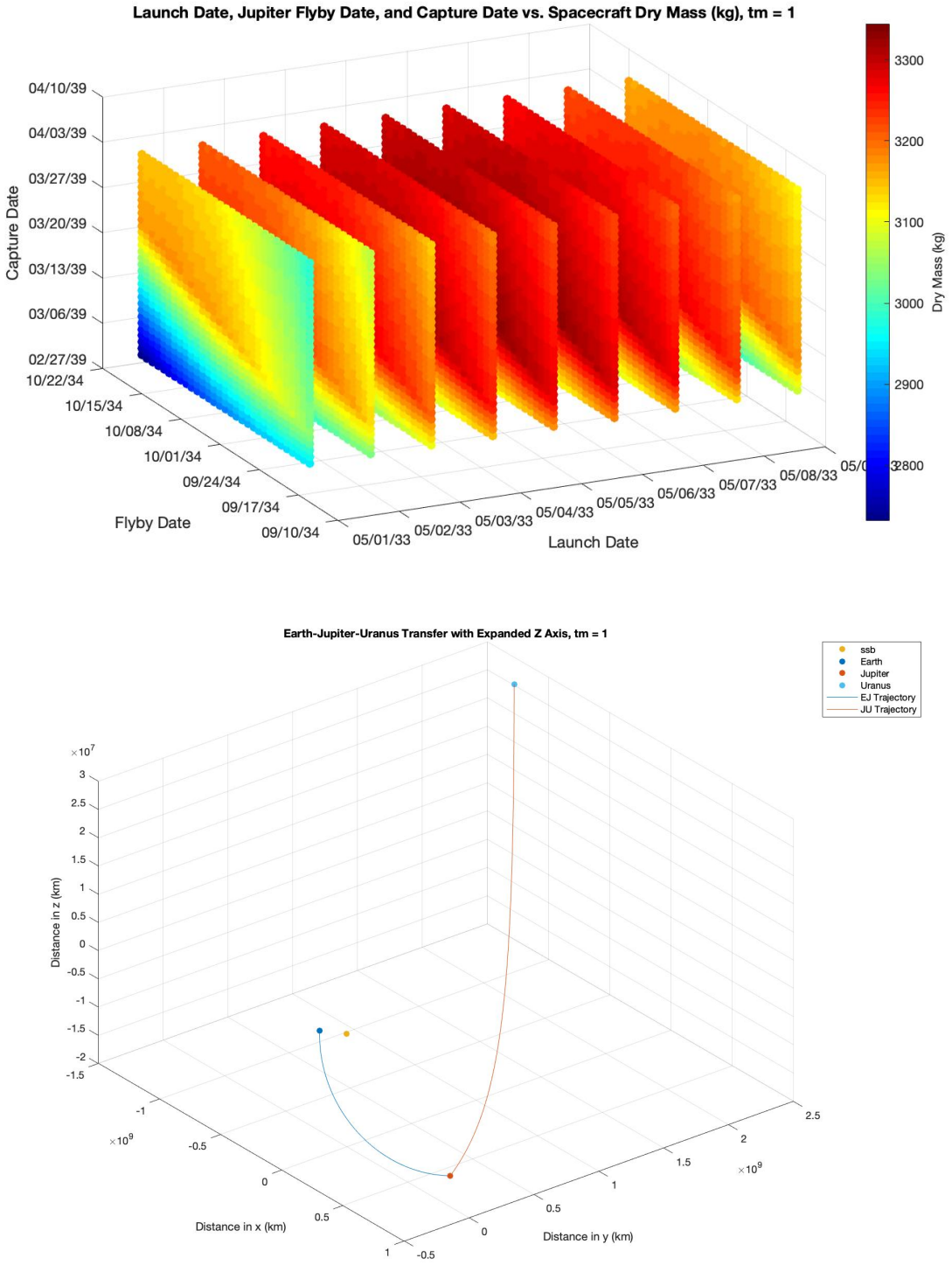

Figure 2.11: Trajectory simulation results for 2033, *tm* 1.

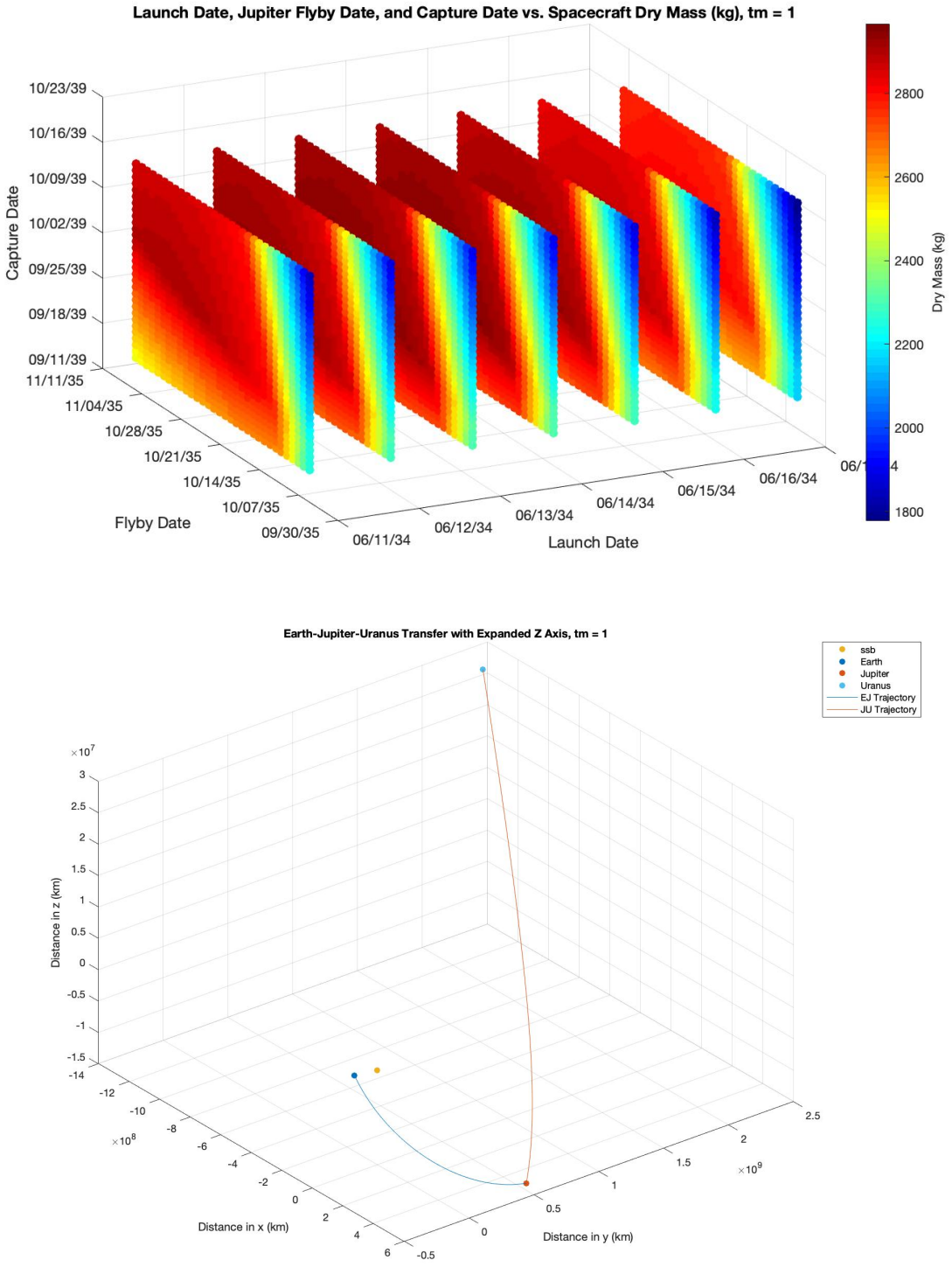

Figure 2.12: Trajectory simulation results for 2034, *tm* 1.

If the spacecraft is launched around May 5th, 2033, using only the excess energy of the launch vehicle, it would reach Jupiter's sphere of influence to perform a powered gravitational slingshot maneuver on October 1st, 2034. The periapsis of the slingshot would occur at an altitude of about 2.23 million kilometers (approximately 32 Jovian radii [RJ]) from Jupiter's atmosphere and would require an additional ΔV of 1.00 km/s to to perform the powered flyby to redirect the spacecraft to Uranus. Such a maneuver would increase the spacecraft's heliocentric velocity by a factor of 2.00, going from 12.74 km/s to 25.49 km/s, providing the necessary ΔV to reach Uranus on March 18th, 2039. This flyby altitude avoids the majority of the Jovian radiation bands, which are strongest under 5 RJ and have a maximum radius of between 50-100 RJ depending on the solar system environment [15]. We recognize that a 2033 launch date would require an accelerated mission development and fabrication timeline, but it would by far produce the most efficient transfer trajectory of the planetary alignment discussed in the PSADS. However, if it becomes clear that a 2033 launch date is not possible, a smaller, lighter spacecraft than proposed UOP is still valuable, as it would still allow for a shorter transfer time, the use of a less powerful rocket, or in the case of significant delays, that a spacecraft could still reach Uranus in a reasonable time with a less optimal alignment of planets.

Upon arriving at Uranus's gravitational sphere of influence, the spacecraft would perform an insertion burn with a ΔV of 0.0067 km/s to enter into a highly eccentric, highly inclined elliptical orbit of eccentricity 0.8 and semi-major axis of 147,794.5 km (5.83 Uranian radii [RU]). This capture orbit provides a good balance between fuel consumption and orbital placement, having a periapsis of 4,000 km (0.158 RU) above the surface of the planet and an apoapsis of 240,000 km (9.46 RU) above the surface of the planet. Such an orbit provides a wide variety of different perspectives for data collection while also providing time for data transfer and battery replenishment. Ad-

ditionally, because the orbit is highly inclined, the spacecraft will be able to image the entirety of Uranus over multiple orbits.

Interestingly, the planetary alignment is such that viewing the solar system from above the ecliptic in the early 2030s presents the thought that one could plan a trajectory to Uranus by executing what is effectively a three dimensional Hohmann transfer with Jupiter and then use the gravity slingshot to arrive at Uranus using less fuel than is proposed above, similar to the simplified trajectory shown in Figure 2.2. However, due to the positions of the Earth, Jupiter, Uranus, and the solar system barycenter (SSB) in the z-axis, such a trajectory is unfeasible, as it would require a trajectory that does not align with the Sun, and therefore would require thrust against the Sun's gravity throughout the transfer. This is much more visible in the expanded z-axis plots shown in Figures 2.3-2.12, rather than a true space depiction, as seen in Figure 2.13.

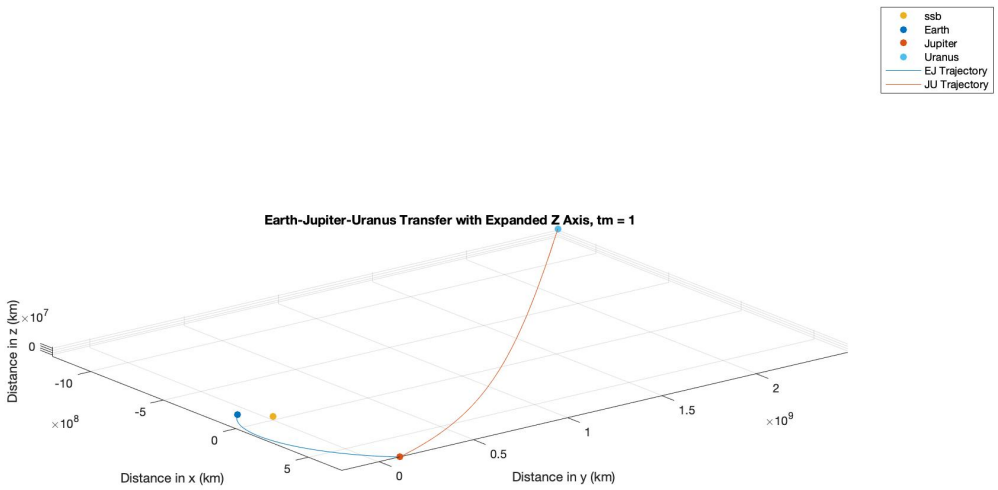

Figure 2.13: True-space trajectory simulation plot for 2033, *tm* 1. Compare this to 2.11 .

It is also worth noting that the C3 for the trajectories optimized for dry mass are high, being around the mid 90s km^2/s^2 when compared with the theoretical optimal

C3 for an EJ Hohmann transfer, which is around 77 km^2/s^2. This can be seen visually in Figure 2.14, which shows the C3 instead of the dry mass for the same launch, flyby, and arrival dates as Figure 2.11. This is because, as with most cases in spaceflight, a lower mass spacecraft is able to execute more efficient burns. Thus, the trajectory is optimized to use as much energy as possible from the launch vehicle in the form of C3, burn harder around Jupiter, and barely burn at all to complete the capture maneuver around Uranus, something that can be seen with the ΔVs of the planned maneuvers.

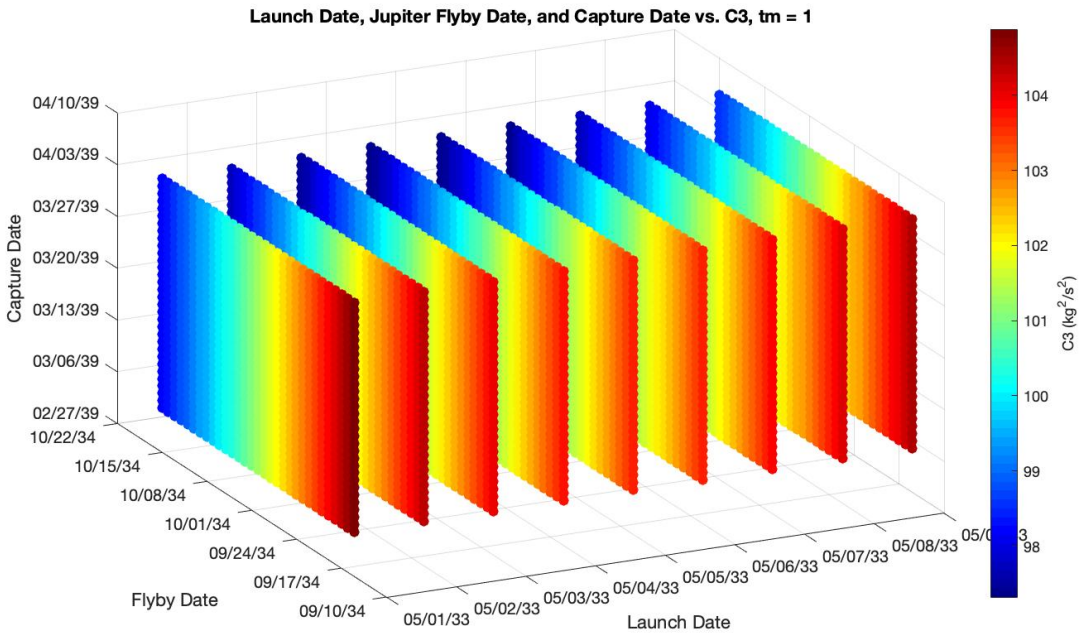

Figure 2.14: C3 values for trajectory simulation results for 2033, *tm* 1. Compare this to 2.11

.

2.3 Concept of Operations

A Concept of Operations, or ConOps, is a mission "plan" that takes into account the mission objectives, science instruments, and all budgets created. It details the factors

that drive mission design, allowing for an iterative design process in conjunction with the technical budgets. At the pre-phase A stage this is more of a high-level overview than an extremely specific plan, but it still provides valuable oversight. The ConOps can be seen in Figure 2.15.

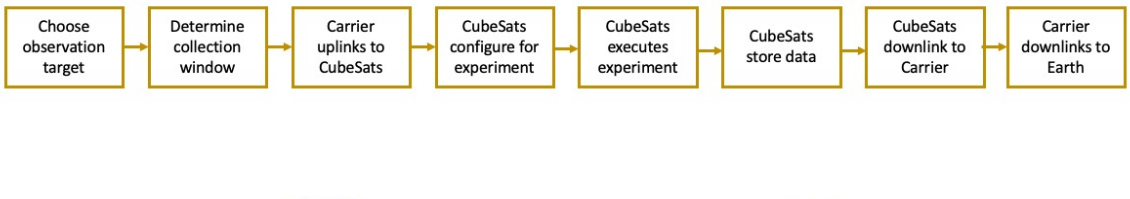

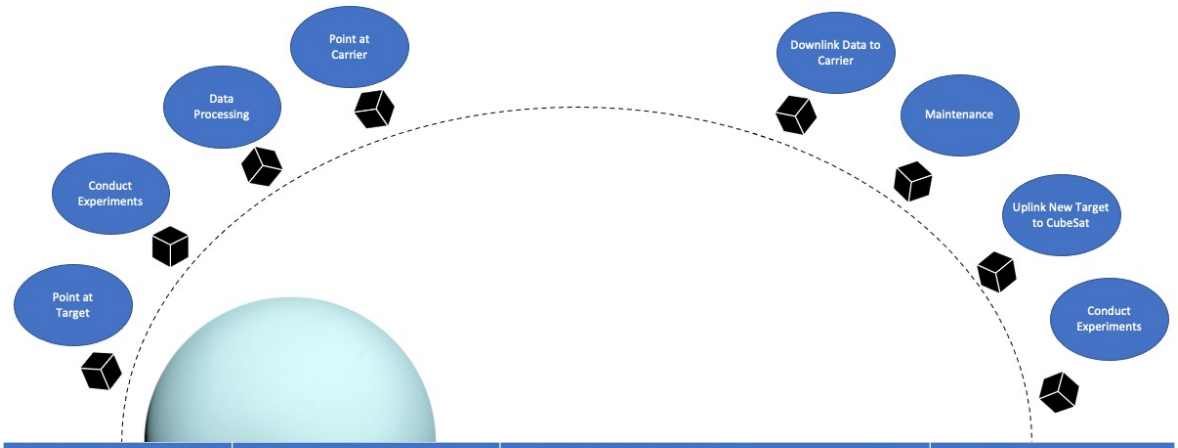

Phase 1: Launch and Cruise (May 3033 – March 2039)	Phase 2: Uranus Arrival and CubeSat Deployment (May 2039 – ~Sept. 2039)	Phase 3: Mission Operations (~Sept. 2039 – ~Sept. 2043 and beyond)	Phase 4: Decommissioning (End of Life)
• Carrier escapes Earth's gravity using the characteristic energy of a launch vehicle • Carrier hibernates until Jupiter Flyby • Carrier performs powered flyby of Jupiter • Carrier hibernates until Uranus arrival burn	• Carrier performs arrival burn • Carrier performs system diagnostic and prepares for CubeSat deployment • Carrier deploys the CubeSats of the preferred groups, with a delay in between releases. • CubeSats are initialized and prepared for mission operations	• Carrier receives observation targets from Earth • Carrier uplinks target to the appropriate CubeSat group • CubeSats point at targets, perform experiments, and record data • CubeSats point at carrier, downlink data, and perform station keeping, power recouperation, and other maintenance • Carrier downlinks data to Earth • Used CubeSats are decommissioned and sent to phase 4, while new CubeSats are launched when needed.	• Group D is decommissioned early and enters atmospheric plunge, transferring as much data as possible to the carrier • Other CubeSat groups begin end of life procedures • Carrier begins end of life procedures

Figure 2.15: ConOps. Gives details about the proposed mission timeline, steps, and operations cycle.

Within the ConOps we detail our nominal mission operation cycle and a high level mission timeline. The nominal mission operations cycle is centered around communi-

cations with Earth through the carrier spacecraft. The cycle begins when the carrier receives an observation target and appropriate collection window from Earth. It will then uplink that data to the appropriate CubeSats. The CubeSats will configure for the experiment and execute it, collecting the data. The CubeSats will then downlink the data back to the carrier spacecraft, which will downlink it to Earth. When not performing an experiment or transferring data, the CubeSats will be performing maintenance or be in a standby mode. Maintenance includes station keeping and recharging the battery after a high-draw task, for example.

The high level mission timeline detailed in the ConOps shows the major steps between the proposed launch in 2033 and end of life/decommissioning, and is split into phases. Phase 1 is the launch and interplanetary cruise. Major events include the escape from Earth's gravity well, the powered Jovian flyby, and the arrival at Uranus. Phase 2 includes Uranus arrival and initial CubeSat deployment. This involves the capture burn to get into orbit around the planet, diagnostic routines, and the deployment of the CubeSats used in the initial experiments. Phase 3 is the mission operations phase, where the spacecrafts are actively performing observations. This involves constant communication with Earth and the mission operation cycle detailed above. As individual CubeSats approach their end of life after a projected lifetime of six months to one year, they move on to phase 4 while new CubeSats are launched from the carrier. Finally, phase 4 is the decommissioning of the spacecraft. CubeSat group D will be the first to decommission, as they are to perform atmospheric plunges. This will require the undivided attention of the carrier spacecraft to maximize the data gathered. After group D has been decommissioned, the other CubeSat groups follow with equal priority. When all CubeSats are decommissioned, the carrier spacecraft will be the final spacecraft to shut down.

2.4 Science Traceability Matrix

A Science Traceability Matrix (STM) is typically needed to translate the mission science objectives into the list of required instruments. The focus of this work is to show that achieving valid scientific objectives is something a swarm of CubeSats could do. Hence, we are not designing the instruments that would go onboard the spacecraft, nor are we characterizing instruments requirements or performance. Our goal is to show that certain types of instruments that could answer the science goals would fit with the available size, weight, and power of a CubeSat bus. As a consequence, we are purposefully omitting some columns of typical STMs, like instrument requirements and projected performance. Our truncated Science Traceability Matrix (tSTM) only includes the science objectives, the physical parameters that need to be determined for the science objective to be answered, and their associated observables. The tSTM is shown in Table 2.2 and summarized in the paragraphs below. Finally, note that the third column lists potential instruments that could be used to measure the associated observables, not necessarily instruments that have already flown onboard CubeSats.

To study the interior composition of Uranus and its ice-rock ratios, a combination of in-situ sampling and remote sensing is necessary. This mission would simultaneously investigate the internal chemical processes, vertical mixing, and dynamic transport over different scales, ranging from milliseconds to days.

To investigate Uranus's atmospheric structure, dynamics, climate, circulation, and meteorological patterns, we will determine the vertical mixing by measuring deep vortices, storms, wave patterns, and non-equilibrium species distribution. Measurements of the dynamics and rotation rates of Uranus through time-dependent mapping of gravity and magnetic fields, radio occultations, and planet seismology will also be performed and used as inputs into comprehensive deep circulation models. This mission

will also investigate stratosphere interactions and their correlation with the planet's seasons through measurements are multiple time scales, ranging from milliseconds to days. Finally, imaging at multiple ranges of wavelength (from infrared to ultraviolet) and radio measurements will determine the characteristics of not only the cloud top but also lower layers of the atmosphere and the convective movements between those layers.

To measure the composition, structures, and geologic history of the moons and rings of Uranus, we will catalogue small moons and fine structures of the rings, measure spectra from the moons and rings in a variety of wavelengths from near infrared to near ultraviolet. We will explore the internal composition of the larger moons through magnetic sounding and gravitational investigations. Finally, we will map the topography and the variations in spectra of the moons through imaging in multiple frequencies.

To understand the magnetosphere and ionosphere of Uranus, the mission will perform particle and field measurements, coupled with simultaneous aurora optical and thermal observations. The spacecraft will also measure the ionospheric composition changes using magnetospheric plasma analyses and ion/neutral composition measurements. To analyze the thermospheric and ionospheric variations and thermal properties of Uranus across different latitudes and time frames, we will use radio occultations, infrared, and ultraviolet spectral limb scans.

To determine how Uranus interacts with its environment, moons, and rings, the effects of tidal dissipation on Uranus's angular momentum will be measured through satellite orbital acceleration. External factors, from micrometeoroids to comets, affecting Uranus's atmospheric chemistry and dynamics will be monitored through time-series imaging and spectral data. Additionally, the influence of seasonal solar insolation on Uranus's atmosphere will be analyzed by using long-term data on temperature, haze, and gas levels. This approach offers valuable insights into the processes governing this

remote gas giant's behavior.

Science objectives	Science Measurement Requirements	
	Physical Parameter	Observables and Potential Instruments
Measure the internal composition of Uranus.	Chemical composition, thermal emissions, optical emissions, high-energy emissions, radio emissions, gravitational fields.	**In Situ and Remote Sensing for Composition:** Spectrometry (Optical & X-ray), Mass Spectrometry, Particle Detectors, Neutron Spectroscopy, Plasma Sensor **Gravity Field Measurements:** Superconduction Gravimeters, Accelerometers, Doppler Shift, Radiometric Tracking, Differential Spacecraft Acceleration
Measure the atmospheric structure and dynamics of Uranus.	Deep vortexes, storms, wave patterns, non-equilibrium species distribution, time-dependent mapping of gravity and magnetic fields, radio occultations, and seismology.	**Vertical Mixing:** Infrared Spectroscopy **Internal Dynamics:** Gravimeter, Magnetometers, Magnetic Resonance Spectrometers
Measure the climate, circulation, and meteorological patterns of Uranus.	Multiwavelength emission of cloud tops and lower atmospheric layers at local and global scales and at short and long time scales.	**Multiwavelength Remote Sensing:** Cameras, Spectrometers, Radiometers, and Photometer **Meteorology:** Spectrometer, Radiometers, Imagers, Mass Spectrometers, Infrared Spectrometer, Anemoeter, Radiosondes, Barometers
Determine what processes lead to the structure, content, and dynamics of Uranus's magnetosphere and ionosphere.	Plasma, particle, and magnetic field observations, ion/neutral composition measurements, thermal properties at various latitude and altitudes in Uranus across latitudes.	**Ionospheric Measurements:** Mass Spectrometer, Magnetometer, Radio Occultation, Spectral Scans, Particle Detectors (Solid-state, Scintillation, Gas), Caloriemeter, Electrostatic Analyzer **Thermospheric Measurements:** Spectrometers, Spectrophotometers, Radiometers, Infrared sensor, Plasma sensor, Langmuir probes, Ion drift meters
Determine how Uranus interacts with its environment, moons, and rings.	Tidal dissipation on Uranus's angular momentum, micrometeoroid and comet impacts, influence of seasonal solar insolation on Uranus's atmosphere.	**Planetary Tidal Dissipation:** Accelerometers, Gravimeters, Radio tracking, Time-series imaging and spectral data

Table 2.2: The truncated Science Traceability Matrix shows how the science objectives are related to potential instruments that would compose the payload of the CubeSats in this mission.

Chapter 3

Spacecraft Design

3.1 CubeSat Design

3.1.1 Overview

As mentioned in Chapter 2, we plan to use a CubeSat swarm to carry the instruments to collect data during this mission. Specifically, we propose to send a 2,360 kg wet mass carrier spacecraft with 16 individual 27U CubeSats (a U, meaning Unit, is a standard measurement of volume used when discussing CubeSats, being equal to 1 dm^3, or 1 liter), each weighing 40 kg wet mass for a total CubeSat wet mass of 640 kg. Each CubeSat contains its own subsystems and is a fully functioning, independent spacecraft in all ways except its ability to communicate with the Earth, as it communicates with the carrier using a dedicated antenna. The carrier then downlinks the data to Earth, effectively treating the carrier as a communications relay to boost the transmission power and gain. A schematic representation of a carrier and 16 27U CubeSats is shown in Figure 3.1, and a basic CAD drawing of a CubeSat with its antenna deployed can be seen in Figure 3.2.

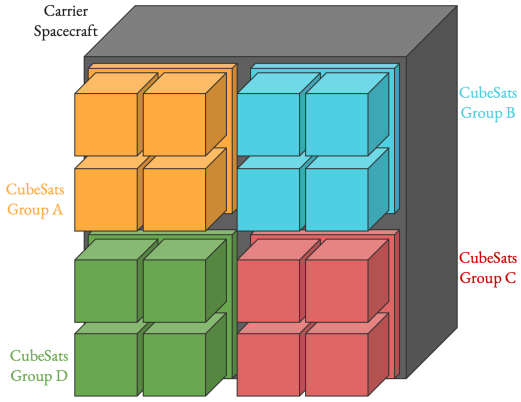

(a) Schematic representation of the Carrier Spacecraft/CubeSat concept.

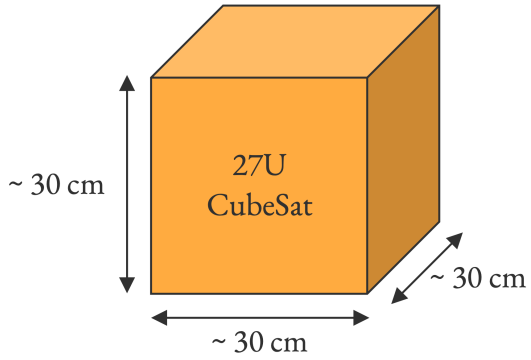

(b) Schematic representation of the 27U CubeSats.

Figure 3.1: Visualization of CubeSats and Carrier Spacecraft

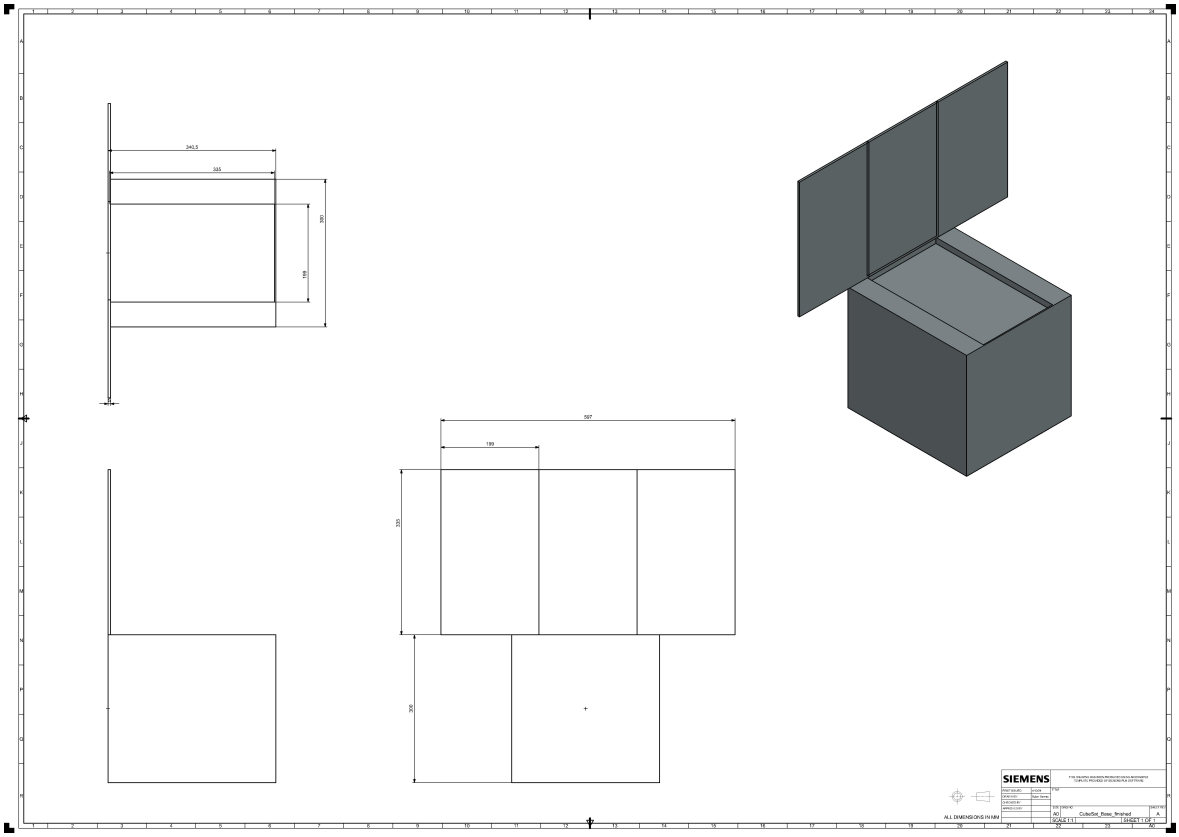

Figure 3.2: Preliminary CubeSat Model and Engineering Drawing

.

3.1.2 Payload

While our main goal is to develop a bus concept that could be suitable for an array of different instruments (which would be selected in the future), it is useful to have examples of instruments for the purposes of visualizing what effects they might have on the design of the spacecraft. As such, we have selected a shortlist of possible instruments from the Cassini cassinimission spacecraft and other planetary science missions as, like them, this mission aims to answer questions about the formation and evolution of planetary bodies of the outer solar system. We chose Cassini as our main comparison point, rather than New Horizons or another more recent mission, as it studied a gas giant, which is more similar to an ice giant like Uranus than a rocky body like Pluto. This shortlist can be seen in Table 3.1.

Acronym	Name	Mission
INMS	Ion and Neutral Mass Spectrometer	Cassini
UVIS	Ultraviolet Imaging Spectrograph	Cassini
GRS	Gamma Ray Spectrometer	Odyssey
CIRS	Composite Infrared Spectrometer	Cassini
MAG	Magnetometer	Cassini
OTD	Optical Transient Detector	MicroLab-1
RPWS	Radio and Plasma Wave Science	Cassini
CAPS	Cassini Plasma Spectrometer	Cassini
VIMS	Visible and Infrared Mapping Spectrometer	Cassini
MKI	Microwave K-band Instrument	GRACE
MIMI	Magnetospheric Imaging Instrument	Cassini
ISS	Imaging Science Subsystem	Cassini/Huygens

Table 3.1: Shortlist of possible instrumentation for a mission to Uranus, sourced from similar planetary science missions in the past. [54, 36, 51, 48]

From this shortlist, we selected four instruments that are most likely to be applicable to answering a wide variety of questions [11]. Because none of the selected instruments are CubeSat sized, we make a comparison between the instruments that have flown on previous missions and Commercial-Off-The-Shelf (COTS) instruments that have CubeSat flight heritage, understanding that the true instruments that would fly on

this mission would likely be somewhere between the two extremes in terms of mass and power requirements. This is because most COTS components are not built to meet the requirements of a planetary science mission other than Earth observation. Our comparison can be seen in Table 3.2, where a historical instrument is described with a COTS equivalent shown below it.

Instrument	Power Requirements W	Mass kg	COTS or Historical
MAG [54]	3.1	3.0	Historical
Magnetometer (3) [4]	1.3 - 3.0	0.3	COTS
CAPS [54]	14.5	12.5	Historical
Plasma Sensor [20]	5	0.1	COTS
Huygens SSP [85]	10	4.2	Historical
Anemometer [80]	0.5	<1*	COTS
CIRS [54]	26.4	39.2	Historical
Multispectral Imager [25]	2.6-4.6	0.5	COTS
MKI [54]	>3*	3.0	Historical
K-band Transmitter [63]	2	1	COTS

Table 3.2: Comparison of traditional deep space instruments to CubeSat sized alternatives.
∗When precise information was not found, bounding values were estimated by the authors.

As per Section 3.1.1, we propose grouping the 16 CubeSats into four groups of four, with each group being specified around one type of data being collected and, therefore, around specific instruments. Group A contains the CubeSats studying the magnetosphere and charged particles, and thus are equipped with the three magnetometers and a boom to reduce interference, along with a plasma sensor to characterize loose ions. Group B studies composition remotely through a multispectral imager. Other possible instruments would be other kinds of cameras or a spectrometer. Group C is comprised of the CubeSats measuring gravity and thus studying the interior of the planet and moons. These measurements would be taken similarly to those of the GRACE mission, which used a K-band radio link with another satellite to measure the slight accelera-

tions due to local gravity anomalies. These two satellites must be on the same orbital plane and around 100 km apart, making CubeSats a natural choice. Thus, this group is equipped with an additional K-band radio and antenna in addition to the radio and antenna used to communicate with the carrier spacecraft. [49] Finally, Group D is built to do atmospheric plunges, diving into the atmosphere and collecting in situ atmospheric samples before breaking down, and therefore has a hot wire anemometer, utilizes the accelerometers in its ADCS system as instruments, and will also use its radio to calculate Doppler shift. Because group D is built for atmospheric plunges, it would likely have a different form factor than the other groups, with some form of passive stability in an atmosphere built into the structure to reduce tumbling as much as possible, similar to the Huygens probe. This, however, would require a custom deployer, which is discussed in section 3.2.

3.1.3 Attitude Determination and Control System

The two key performance measures of the CubeSat's Attitude Determination and Control System (ADCS) are its ability to point at the carrier spacecraft with little enough error to transmit and receive a signal and its ability to stay focused on a single point on Uranus at any time to be able to accomplish the desired scientific measurements. Before calculating those performance measures, however, we must first calculate our pointing budget, which is presented in Table 3.3. The budget results in a maximum slew rate of 1.03 $^\circ/s$ and a maximum angular acceleration rate of 0.10 $^\circ/s^2$.

To calculate the ability to point at the carrier spacecraft correctly, we compare the angular error in the pointing budget to the angular beam width of the CubeSat's antenna. The CubeSat's antenna has a beam profile such that most of the power is within $\pm$ 10° of the direction it points [32]. When this is compared to the error value of 0.01°, we see that the carrier will easily be within the beam of the antenna. The

Error Source	Error Value (°)	Error Value (m)
Position Knowledge Error	0.008400	35772.27
Mechanical alignment	0.000278	1182.95
ADCS	0.001667	7097.67
Thermal	0.000833	3548.84
Totals	0.011178	47601.72
Inputs		
Characteristic	Value	Unit
Range (km)	244000	km
Range Knowledge Error	0.001	km
Momentum storage	0.0108	Nms
Torque	0.001	Nm
High Moment of inertia	0.60	kg-m2
Momentum Results		
Characteristic	Value	Unit
Max Slew Rate	1.03	°/s
Max Angular Acceleration	0.10	$°/s^2$

Table 3.3: CubeSat Pointing Budget Summary. It is worth noting that most of the error comes from position uncertainty, rather than an error in angle.

sensors used for ADCS are two star trackers, a horizon sensor, and a three-axis inertial mass unit (IMU), collectively labeled under GNC sensors in other budgets.

To calculate if the spacecraft can stay pointed at a single spot on Uranus at any time, we look at the most severe case, which is when the spacecraft is at periapsis looking toward the center of the planet. If the angular velocity of the spacecraft at that point is less than or equal to the maximum slew rate, the spacecraft can focus on any one point at any point in the orbit. To calculate the angular velocity, we use Equation 3.1, the *Vis-Viva* equation, to get the spacecraft's velocity at periapsis.

$$v = \sqrt{\mu \left(\frac{2}{r} - \frac{1}{a} \right)} \tag{3.1}$$

Where v is the velocity (which at periapsis is only the tangential velocity component as there is no radial velocity), mu is the standard gravitational parameter of Uranus, r is the distance from the planet's center of mass, and a is the semi-major axis of the

orbit. From this equation, we get that the spacecraft's velocity is 20.0 km/s. As stated in Section 2.2, the altitude at periapsis is 4,000 km, so we can calculate the angular velocity with Equation 3.2.

$$\omega = \frac{v}{h} \tag{3.2}$$

Where ω is the angular velocity, and h is the orbital altitude. We find the angular velocity at periapsis to be 0.005 radians/s or less than 0.3 °/s, which is less than the maximum slew rate of 1.03 °/s. This means that the pointing budget closes, and the CubeSats are capable of pointing for both science and communication purposes.

3.1.4 Communications

The communication system presents a unique challenge when designing a CubeSat, as spacecraft communications are often one of the most power-intensive subsystems of a mission [84], and antenna size is directly related to signal strength [9]. As CubeSats are generally designed to be small, low-power spacecraft, these challenges leave them at a disadvantage when compared to traditional spacecraft. However, it is possible to overcome these design challenges through the use of carefully selected hardware and engineering budget calculations.

The first important point to recognize is that a CubeSat on its own is unable to communicate with the Earth when in orbit around Uranus. This led to the decision to use the carrier spacecraft as a communications relay, drastically shortening the distance across which the CubeSats would have to transmit. However, even with this reduction, the CubeSats will still be required to transmit across, at maximum, the full major axis of the Uranus capture orbit, which is a distance of almost 300,000 km. This is made more difficult as most CubeSat-sized radios have a maximum output of around 2 W,

which is insufficient to transmit that distance, even when using a high-gain antenna.

We mitigate this issue through several factors. First, we recognize that if the CubeSat was attempting to transmit at its true boundary case of the major axis, Uranus would be in the middle of the transmission line and completely block the signal. Because of this, we can reduce the transfer range by about the diameter of Uranus, which is 50,000 km. Second, we can increase the power of the CubeSat's radio by adding an amplifier to increase the transmission power to 5 W. Thirdly, we can add a low noise amplifier to the receiver on the carrier spacecraft, effectively boosting the signal-to-noise ratio. Finally, we can recognize that a similar problem has already been solved. The MarCO CubeSats were required to communicate between the Earth and Mars, and in doing so ran into a similar challenge. The solution was an antenna designed for a CubeSat form factor but having a gain an order of magnitude higher than the best COTS antennas for CubeSats [32]. All of these factors lead to a converging solution with modern, flight-tested hardware. A breakdown of the communications budget for a worst case (longest distance) scenario can be seen in Table 3.4. This link closes with a margin of 7.2 dB, which is more than our required 6 dB minimum margin.

Moving on to the data budget, as we are not proposing specific instruments but rather using general types of instruments as examples, any data budget created with a specific instrument in mind may differ greatly from what we describe in this section. That being said, two data budgets have been created for the A and B CubeSat groups as detailed in Section 3.1.1, which are the magnetometer and multispectral imager CubeSats, respectively. The data collection characteristics for these instruments were based on the MAG instrument from Cassini [47] and the RALPH MVIC instrument from New Horizons [68]. Each image from MVIC is 964,608 bytes. A full breakdown of the data budget over one day for group A can be seen in Table 3.5, while a results summary for group B can be seen in Table 3.6.

General Information		
Characteristic	Value	Unit
Distance	244000	km
Transmitter Information		
Characteristic	Value	Unit
Frequency	8.425	GHz
Bit rate	0.100	Mbps
Transmit Power	5.0	W
Transmit Power	37.0	dBm
Transmit antenna gain	29.2	dBi
Transmit system losses	-4	dB
EIRP	62.2	dBm
Path loss	-218.71	dB
Receiver Information		
Characteristic	Value	Unit
Receive antenna diameter	0.5	m
Antenna Efficiency	80	%
Receive antenna gain	31.9	dBi
Receive amplifier	13.0	dBi
Noise Temperature	150.0	K
Receive system noise figure	-176.84	dBm/Hz
Total Received Power	-107.6	dBm
Receiver system losses	-4	dB
Cross polarization loss	0	dB
Link Margin Computation		
Characteristic	Value	Unit
Received Eb/No	15.2	dB
Required Eb/No	8.0	dB
Link margin	7.2	dB
Required link margin	6	dB

Table 3.4: CubeSat Link Budget Summary. The link margin is 7.2 dB, whereas the required link margin is 6 dB, showing the convergence of the budget.

Group A					
Subsystem	Description	Size (Bytes)	Sample Total (Bytes)	Overhead (Bytes)	Total (Bytes)
CDH	SOH (State of Health)	86400	2,246,400	72,412	2,318,794
EPS	SOH (State of Health)	86400	4,838,400	155,943	4,994,325
ADCS	SOH (State of Health)	86400	1,900,800	61,274	1,962,056
PAY	SOH (State of Health)	86400	1,123,200	36,215	1,159,397
ADCS	Reaction wheel Data	86400	1,641,600	52,921	1,694,503
ADCS	Sensor Data	86400	3,283,200	105,824	3,389,006
THM	RTD Data	86400	2,073,600	66,843	2,140,425
EPS	Switch Data	86400	684,288	22,070	706,340
EPS	Bus Data	86400	1,728,000	55,706	1,783,688
PAY	Magnetometer	86400	30,585,600	985,687	31,571,269

Inputs		
Characteristic	Value	Units
Pass Time	360	minutes
Number of passes in a day	1	pass
Radio Data Rate	100000	bps
Total number of images for experiment	10	images
Margin	33	%

Results		
Characteristic	Value	Units
Number of passes to downlink all data	1	passes
Number of days to downlink all data	1	days
Total Bytes Generated (1 Day)	51,719,803	Bytes
Total Bytes with Margin	68,787,338	Bytes
Total (kB)	67,175	kB

Table 3.5: Data Budget Summary for magnetometer CubeSat group. The summary shows that each CubeSat required one pass to downlink all data, which is a good result. Sample overhead and downlink overhead were combined into one column simply titled Overhead.

Group B		
Characteristic	Value	Unit
Number of images for experiment	25	images
Number of passes to downlink all data	1	passes
Number of days to downlink all data	1	passes
Total Bytes Generated (1 Day)	45,041,349	Bytes
Total Bytes with Margin	59,904,994	Bytes
Total (kB)	58,501	kB

Table 3.6: Data Budget Summary for multispectral imager CubeSat group. The summary shows that each CubeSat required one pass to downlink all data, which is the best possible timeframe.

3.1.5 Power

Because this mission operates beyond Jupiter (5 AU), using solar power would be extremely limiting for our power budget. Thus, we choose to rely on nuclear power. Previous deep space missions have used Radioisotope Thermoelectric Generators (RTGs), or in more recent years, multi-mission Radioisotope Thermoelectric Generators (MMRTGs) that provide on the order of 110 W while occupying 212 L volume and 45 kg, which are far too large for CubeSats [52].

Instead, we propose using an emerging technology, the thermoradiative cell (TRC) [82]. A TRC generates electricity by taking advantage of a temperature gradient, such as that between a nuclear heat source and the vacuum of space. It is more efficient than an MMRTG, having an order of magnitude increase in mass specific power (producing $\sim$30 W/kg vs the $\sim$3 W/kg typically produced by RTGs) and using only 0.2 liters of space[65] — a three orders of magnitude decrease in volume. This makes the TRC far more accessible for smaller spacecraft, such as CubeSats. TRCs do not have flight heritage yet, but the technology is quickly evolving and could be ready for use by the time a Uranus mission gets into the detailed design stage.

To provide the heat that the TRC requires for producing electricity, we propose using two individual General Purpose Heat Sources (GPHSs). These are the same nuclear heat sources inside the RTGs and MMRTGs that have launched previously on other missions, with one MMRTG containing eight GPHSs. As each GPHS generates $\sim$250 W of heat, we can calculate that the TRCs will generate $\sim$33.86 W of electricity. It is worth noting that since we are proposing to launch 16 CubeSats, we would be using 32 GPHSs, which is the equivalent of four MMRTGs (without considering another MMRTG for the carrier spacecraft). This is a significant amount of radioactive material, especially considering that New Horizons, one of the most recent deep space missions, only used one MMRTG, and Cassini only used three GPHS RTGs. We also

understand that GPHSs are not yet certified for this configuration, which would be another time-limited objective. We understand that there are multiple cost, timeline, and political implications of requiring such a large number of GPHSs. However, given how far Uranus is from the Sun, using nuclear power is the only way in which a swarm of CubeSats could be feasible with the currently available technology.

Baseline Operations		
Component	Power Contribution W	Group
Generator (GPHS & TRC)	+33.861	Universal
GNC Sensors [57]	-3.7	Universal
Reaction Wheels (4, avg) [22]	-0.76	Universal
Computer [55]	-10	Universal
Memory (2) [55]	-0.6	Universal
Clock [57]	-1.5	Universal
Heaters [78]	-10	Universal
Total	+7.301	
Short Term Operations		
Radio [56]	-2.6	Universal
Amplifier [56]	-8	Universal
Cold Gas (6) [46]	-<63	Universal
Reaction Wheels (4, peak) [22]	-9.2	Universal
Group Specific Components		
Plasma Sensor [20]	-5	A
Magnetometer (3) [4]	-3	A
Multispectral Imager [25]	-4.6	B
K-Band Transmitter [63]	-2	C
Anemometer [80]	-0.5	D

Table 3.7: Power budget summary. Components in all CubeSat groups that run constantly are under baseline operations. Components in all CubeSat groups that are only engaged short term or have a peak power draw significantly different from the average power draw are under short term operations. Finally, instruments or other components which are only part of one group are under group specific components.

In addition to the power generation, we also propose a battery to act as a buffer for high power draw operations, such as data transfer or thruster firing. As a preliminary design, we have sized and accounted for a lithium-ion battery that holds two hours of

standard power consumption. A summary of the power budget can be seen in Table 3.7. Regular baseline operations can be seen in the first section of the table, while any component that is either not regularly engaged or has a significantly different peak power consumption compared to standard operations can be found in the Short Term Operations section. Finally, any component that differs between different groups of spacecraft can be seen in the group specific section with their group listed.

3.1.6 Thermal

Because the only method of heat transfer with the environment in space is radiation, and with the goal of finding the worst-case scenario of maximum heat loss, we approximated the heat loss by considering the spacecraft as a black body that absorbs no radiation and emits at the optimal temperature range of a lithium-ion battery. As we are treating the spacecraft as a black body, we can use the Stefan-Boltzmann Law, shown as Equation 3.3, to determine the thermal energy lost as radiation at any given temperature.

$$P = A\epsilon\sigma T^4 \tag{3.3}$$

Where P is power lost, A is the surface area, which for a standard 27U CubeSat is $0.54m^2$, ϵ is the emissivity, which for a black body is 1, σ is the Stefan–Boltzmann constant, and T is the absolute temperature of the emitter. Taking the optimum temperature range of a lithium-ion battery as the working range (10 °C - 30 °C) as it is the most temperature-sensitive component on the spacecraft, we can calculate that we will lose a maximum of 197 W at 10 °C and 259 W at 30 °C.

As discussed in Section 3.1.5, we use two GPHSs to generate heat, totaling 500 W of thermal heat being generated. Of those, 33.86 W gets directly converted into electricity,

leaving the question of how much heat is radiated away into space by the TRCs and how much is maintained by the spacecraft. Assuming that thermoradiative cells have a similar efficiency to solar panels, we retain 30% of the waste heat, meaning that we retain around 140 W of waste heat, which is outside of the working range defined by the lithium-ion battery. However, this is only the case if we were to attempt to maintain a uniform temperature throughout the entire CubeSat within the battery's temperature range. We understand that internal temperature is not a constant in spacecraft outside of theory and that, in reality, there are additional effects, such as planetshine and albedo, but this analysis shows a workable result for a preliminary thermal calculation.

To account for the fact that internal temperature is not a constant in spacecraft, we plan to primarily use passive thermal control, as we are concerned with managing the heat we already have, so we have to generate as little as possible. However, we will likely still need some form of active heat control to regulate the temperature of the electronics or thruster lines. In this iteration of our design, we propose using Kapton heaters [78] as recommended by [58] with a capacity of 10 W. This is an initial number pending computational thermal analysis. There is also the option of using radioisotope heater units (RHUs), which provide 1 W each. They are heavier than electronic heaters but require no electricity.

3.1.7 Structures

We found that CubeSat mass and volume were not limiting factors in this design, given that CubeSat sized parts are being used. The full mass and volume breakdown can be seen in Table 3.8, which shows that the mass margin is 18.1 % and the volume margin is 34.9 %.

While the mass and volume budgets close, the volume by a large margin, the final

mass budget margins is lower than is optimal for this point in the design. However, it's worth noting that there is excess launch mass available, as shown in section 3.2, and thus the CubeSats' weight allowances could be increased if necessary.

Universal Components			
Component	Mass (kg)	Size (L)	Group
Generator (GPHS, Shielding, & TRC)	9.383	1.491	Universal
GNC Sensors	0.365	< 1*	Universal
Reaction Wheels (4)	0.6	0.267	Universal
Radio	0.094	0.2	Universal
Computer	1	< 3.125*	Universal
Memory	0.08	< 1*	Universal
Clock [57]	0.016	0.004	Universal
Amplifier	1*	0.0121	Universal
60 Ah Battery	7.23	5.469	Universal
Antenna [32]	1	1.67, undeployed	Universal
Cold gas thrusters (6) [46]	0.420	0.0705	Universal
Fuel tank	0.6	9.819	Universal
Structure	3.6217	27	Universal
Total	24.771	15.572	Universal
Margin	15.229	11.426	
Margin, %	38.1%	42.3%	
Electronics and Harnessing buffer	20% (8 kg)	7.5% (2 l)	Universal
Final margin	7.229	9.426	
Final margin, %	18.1%	34.9%	
Group Specific Components			
Component	Mass (kg)	Size (L)	Group
Plasma Sensor [20]	0.1	0.5*	A
Magnetometer (3) [4]	0.5	0.3	A
Multispectral Imager [25]	0.3	1	B
K-Band Transmitter [63]	1	0.8	C
Anemometer [80]	< 1*	0.125*	D

Table 3.8: Mass and Volume Budget. Shows a summary of masses and volumes of components used in other budgets, as well as the remaining margins compared to the maximum allowable mass and volume.
*When precise information was not found, bounding values were estimated by the authors.

3.1.7.1 Radiation Mitigation

Radiation presents a significant design challenge to any spacecraft, but especially CubeSats, as they generally have less shielding and use fewer radiation hardened components. There are two main sources of ionizing radiation: environmental and internal radiation, both of which can be mitigated through shielding, but also through using radiation hardened or resistant components, both of which raise the total lifetime radiation dose the spacecraft can withstand.

Environmental radiation is primarily mitigated through external shielding, or shielding on the outside of the spacecraft. While in transit to Uranus, the CubeSats are protected by the carrier spacecraft itself, requiring no additional mass on the part of the CubeSat and lowering lifetime radiation dose significantly. Once a CubeSat has been released into orbit around Uranus, however, it must rely on its own shielding. For similar missions, it has been projected that 100 mils (2.54 mm) of aluminum shielding is enough to mitigate radiation for standard, radiation hardened electronics for the lifetime of this mission [6].

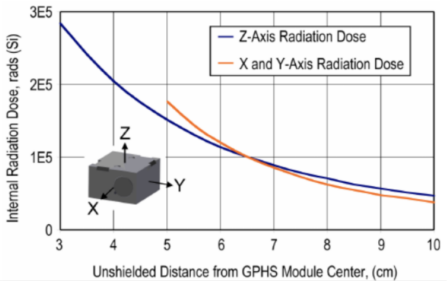

Figure 3.3: GPHS 13-Year Radiation Dose. With a 4.5-year science phase, we assume that the radiation from 13 years will be greater than the lifetime radiation from a six-year transfer and less-than-five-year science phase. [5]

Internal radiation from the decay of the nuclear heat source also needs to be shielded against. This shielding surrounds the heat source, leading to a lower required mass of material than the equivalent external shielding. We used Equation 3.4 to determine the required shielding thickness given the worst case lifetime radiation dose, which we can find from Figure 3.3.

$$I = I_0 e^{-\mu r} \tag{3.4}$$

Where I_0 is the incident radiation intensity, I is the residual radiation intensity, r is the thickness of the shielding material, and μ is the linear attenuation coefficient of the material being used as shielding.

Doubling the maximum radiation dose because of the two GPHSs and assuming no mutual shielding, we can reduce the lifetime radiation dose to 1 krad with an aluminum shield 0.445 cm thick, which is well within the bounds of most components. The mass of the internal and external shielding can be calculated by multiplying the shield thickness by the surface area it is shielding. The total shield mass was calculated to be 5.255 kg. Most other deep-space spacecraft endure much higher lifetime radiation doses. Cassini, for example, was designed such that its sensitive subsystems and instruments were able to withstand 20 krad solely from external sources of radiation [6]. However, CubeSats do not have the same historical testing, and many COTS components that are being used for reference have not been built to be radiation hardened. Therefore, we decide to err on the side of caution in this stage of development.

3.2 Carrier Spacecraft Design

3.2.1 Overview

For this mission, the carrier spacecraft serves two main purposes: to be the method by which the CubeSats are transported to Uranus and the method by which they communicate with Earth. To better fulfill both purposes, the carrier is designed to be a more traditional spacecraft for deep space exploration, especially when compared to the CubeSats, as it needs to have the size and mass to support large and heavy

components, such as RTGs and large antennas, while also being able to contain and deploy all 16 CubeSats which, when arranged as compactly as possible, still take up 0.432 m^3 without any kind of support structure.

3.2.2 Payload

The first requirement of the carrier spacecraft is to provide a bus to secure the CubeSats while they are being transported to Uranus. This involves keeping the CubeSats together inside of their deployers on the carrier throughout the entirety of the interplanetary transfer. Not only does this keep the CubeSats in one plane, but it also protects them somewhat from the challenging environment of space. For example, keeping the CubeSats inside the carrier spacecraft allows them to use the carrier as additional shielding from ionizing radiation and micrometeoroids, giving the CubeSats a longer lifetime once released, as they have not gathered as much lifetime radiation and other types of wear than they would have otherwise. Additionally, by containing the CubeSats within the carrier, we gain access to liquid bipropellant thrusters for the orbital insertion burn and Jovian flyby, which are both more powerful and efficient than the cold gas thrusters on the CubeSats themselves. This means that we require far less fuel to place the spacecraft in the same orbit than we would using the less efficient thrusters. This also allows us to save the propellant in the CubeSats themselves for station keeping and desaturation.

While within the carrier spacecraft, the CubeSats will be contained within their deployers. Traditionally, one of the reasons CubeSats have proliferated so much is the design of the first CubeSat deployer, the Poly Picosatellite Orbital Deployer (P-POD) [16, 40], whose design principles have been passed down to all others. A CubeSat deployer not only allows a CubeSat to be launched into space but also allows a launch provider or CubeSat designer to treat whatever is contained within the deployer as a

black box, as the deployer itself is effectively the bus for the CubeSat. This allows the launch vehicle to be certified for flight separately from the CubeSat, allowing far easier ridesharing. In the case of this mission, no COTS deployer is rated for a 27U CubeSat, as that is significantly larger than other CubeSats launched to this point. However, similar design principles can be used to simply scale up the design of an already flight-tested product. The CubeSats and deployers will be configured in the carrier spacecraft such that a CubeSat from any one design group would be able to launch at any given time, allowing a CubeSat that has already been launched and has reached end-of-life to then be replaced.

Once the spacecraft reaches Uranus's orbit and the carrier spacecraft releases the CubeSats, the carrier transitions into being a communications relay. This design decision is because, as described in Section 3.1.4, a CubeSat does not have the power and antenna gain to transfer data back to Earth directly. Thus, the CubeSats transfer data to the carrier, and the carrier communicates back to Earth. The carrier spacecraft will utilize two separate antenna and radio systems. When communicating with the CubeSats, the carrier uses a dedicated high gain antenna (0.5 m diameter dish) equipped with a different radio to the one it uses to communicate with Earth. This allows the carrier to simultaneously be in contact with the CubeSats and the Earth, increasing the data transfer rate and reducing the amount of energy needed to constantly reorient the carrier spacecraft to change pointing targets. To communicate with the Earth, the carrier would use a larger antenna and a more powerful radio to communicate via NASA's Deep Space Network (DSN) [38] over the X-band, which has been used by many deep space missions, including New Horizons [31]. There is no significant absorption of the X-band by Uranus's atmosphere [42], thus appearing to be a viable frequency range.

At times when the carrier is not utilizing all of its antennas to communicate with

the CubeSats, the carrier could also accomplish science objectives by using the different frequency receivers to study Uranus. The carrier could also carry additional instruments that are too large to be on the CubeSats, but a more detailed analysis is necessary before such a decision can be made. However, any additional mass for the carrier would likely go toward power generation or fuel, thus expanding mission longevity rather than adding instruments to said spacecraft and diluting its purpose.

3.2.3 Bus

3.2.3.1 Communications

In section 3.1.4, we showed that the CubeSats are capable of transmitting to the carrier spacecraft. Here, we will show that the carrier is capable of transmitting to both the CubeSats and the Earth. In the design of the carrier spacecraft communications system, we heavily reference the New Horizons antenna and communications system [72], as it is the most modern spacecraft that has communicated past Jupiter, and because New Horizons has communicated with the Earth from beyond Pluto, the New Horizons system is also able to communicate from Uranus. Given data from the New Horizons antenna and the DSN [77], we can construct the link budget shown in Table 3.9. Like in Table 3.4 this budget is for a worst case scenario, where the communication distances are the longest possible for each pair.

3.2.3.2 Attitude Determination and Control System

While we do not yet have an overall carrier CAD design advanced enough to calculate specific moments of inertia for the ADCS system to use, we can approximate what the pointing requirements of the spacecraft might be. This analysis is shown in Table 3.10

To calculate the ability to point at the carrier spacecraft correctly, we compare

General Information				
	Earth		CubeSats	
Characteristic	Value	Unit	Value	Unit
Distance	3200000000	km	244000	km
Transmitter Information				
Characteristic	Value	Unit	Value	Unit
Frequency	10	GHz	8.425	GHz
Bit rate	0.100	Mbps	0.050	Mbps
Transmit Power	13.0	W	13.0	W
Transmit Power	41.12	dBm	41.12	dBm
Transmit antenna gain	42	dBi	42	dBi
Transmit system losses	-4	dB	-4	dB
EIRP	79.14	dBm	69.04	dBm
Path loss	-302.55	dB	-218.71	dB
Receiver Information				
Characteristic	Value	Unit	Value	Unit
Receive antenna diameter	70	m	0.367	m
Antenna Efficiency	80	%	80	%
Receive antenna gain	76.3	dBi	29.2	dBi
Receive amplifier	30	dBi	5.0	dBi
Noise Temperature	29.2	K	150	K
Receive system noise figure	-183.95	dBm/Hz	-176.84	dBm/Hz
Total Received Power	-113.1	dBm	-111.4	dBm
Receiver system losses	-4	dB	-4	dB
Cross polarization loss	0	dB	0	dB
Link Margin Computation				
Characteristic	Value	Unit	Value	Unit
Received Eb/No	16.9	dB	14.4	dB
Required Eb/No	8.0	dB	8.0	dB
Link margin	8.9	dB	6.4	dB
Required link margin	6	dB	6	dB

Table 3.9: Carrier Link Budget Summary. The link margin is 8.9 dB for communication with the Earth and 6.4 dB for communication with the CubeSats, whereas the required link margin is 6 dB, showing the convergence of the budget.

the angular error in the pointing budget to the angular beam width of the CubeSat's antenna. The carrier uses a high-gain dish antenna and thus has a beam profile such that most of the power is within $\pm$ 1° of the direction it points. Given that the carrier spacecraft has an ADCS sensor suite that is equally as capable as the CubeSats, the dominating error would still be position knowledge error. When this is compared to

Error Source	Error Value (°)	Error Value (m)
Position Knowledge Error	0.008400	469144506.30
Mechanical alignment	0.000278	15514037.80
ADCS	0.001667	93084226.80
Thermal	0.000833	46542113.39
Totals	0.011178	624284884.28
Inputs		
Characteristic	Value	Unit
Range (km)	3200000000	km
Range Knowledge Error	0.001	km
Momentum storage	20	Nms
Torque	30	Nm
High Moment of inertia	5833.33	kg-m2
Momentum Results		
Characteristic	Value	Unit
Max Slew Rate	0.20	°/s
Max Angular Acceleration	0.29	$°/s^2$

Table 3.10: Carrier Pointing Budget Summary. It is worth noting that most of the error comes from position uncertainty, rather than an error in angle.

the error value of 0.01°, we see that the carrier will easily be within the beam of the antenna. The pointing error would have to be on the order of 3500 arc seconds to cause an issue with pointing at the Earth, which is easily avoidable.

As we can choose when to communicate with the CubeSats, we can select points when the angular velocity of the CubeSats relative to the carrier spacecraft will be small enough that communication will be possible, regardless of the carrier momentum control characteristics. However, to achieve somewhat similar values to the CubeSats, approximating the high moment of inertia, the carrier spacecraft would require a momentum storage of 20 Nms and a torque of 30 Nm to get a fifth of the max slew rate. The maximum angular acceleration would double, however.

3.2.3.3 Power

The power source selected for the carrier spacecraft is a full-size RTG. Because we have a form factor that supports its use, we choose to use an RTG over a TRC-based power system to reduce both risk and certifications for new nuclear power configurations. As of the writing of this document, the most advanced RTG under study is the Next Generation Radioisotope Thermoelectric Generator (Next Gen RTG), which is slated to be ready for use in the early 2030s [45]. Initial results suggest that a single RTG could generate 500 W at the beginning of life (BOL) and 362 W after 17 years, which should be sufficient to power this spacecraft when compared to similar spacecraft, such as Cassini or New Horizons. A selection of RTGs is shown in Table 3.11

Metric	System			
	MMRTG	eMMRTG*	GPHS - RTG	NextGen*
Power, BOL (W)	110	150	290	500
Power, EOM (W)	55	91	213	362
Design Life (yrs)	17	17	18	17
Degradation rate	4.8%	2.5%	1.9%	1.9%
# GPHS	16	16	18	16
Length (m)	0.69	0.69	1.14	1.04
Mass (kg)	4 5	44	57	62

Table 3.11: Selection of RTGs, both historical and currently in development. Table from [45]. * Predicted values

3.2.3.4 Structures

While many elements of the carrier spacecraft have not yet been sourced, making a detailed structural breakdown with mass and volume budgets impractical, some general points can be made. The carrier spacecraft was initially sized such that its 2,360 kg wet mass would combine with the CubeSats' 640 kg wet mass to be a total 3,000 kg wet mass spacecraft. However, as analysis advanced, the total spacecraft mass allowance also increased. The current optimum trajectory, per section 2.2, allows for a total

spacecraft wet mass of 4,488 kg, divided into 3,344 kg dry mass (which includes the weight of fuel for the CubeSats, as they are considered payload) and 1,144 kg of fuel for maneuvers. Even adding a 30% fuel margin, bringing the fuel mass up to 1,487 kg, results in a heavier dry mass spacecraft than initial sizing allowed.

This extra mass allowance leads to extra design flexibility. Several examples of possibilities include how CubeSats could be adjusted to have a higher mass limit or their number could be increased, how additional fuel and fuel storage could be added to the carrier or the CubeSats to extend the mission duration, or how scientific instruments that require more space, power, and mass could be added to the carrier spacecraft to gather additional data. As the requirements for this mission change, there is space for the mission itself to also adapt.

Chapter 4

Conclusion

4.1 Summary

This work demonstrates that a CubeSat swarm mission to Uranus is likely a viable solution for answering many aspects of the 2023-2032 Planetary Science and Astrobiology Decadal Survey's thematic questions and can support the UOP by collecting data that the UOP cannot. We have shown that there is a unique scientific benefit to launching a lighter spacecraft on a lower fuel and cruise time trajectory — arriving at Uranus in around six years in an optimal trajectory so that we can observe the shift from the northern solstice to the equinox and thus observing a planet-wide change in climate. This timeline acceleration also results in the ability to take advantage of an advantageous planetary alignment while the UOP Flagship mission likely will not be completed in time to do so, and is a mission with lower complexity, lower personnel upkeep costs, and more potential of high-return scientific mission extensions.

We have shown that a swarm of CubeSats can return valuable data, comparable to a single large spacecraft, using many of the same types of instruments. We also argue that using a swarm of smaller spacecraft presents improvements in coverage and

revisit rates of the planetary surface compared to a traditional spacecraft. Additionally, we have shown that using a swarm allows the distributed system to collect data that would otherwise be inaccessible or much more difficult to obtain, such as mapping the gravitational field of Uranus to a great deal of precision or creating a 3D representation of phenomena by observing it from multiple angles using multiple spacecraft.

We have shown that a carrier spacecraft is a viable method of transporting CubeSats on interplanetary trajectories, allowing the use of more powerful and efficient thrust mechanisms and protecting the CubeSats from the deep space environment. We have also proven that a carrier spacecraft is also capable of acting as a communications relay for the CubeSats to communicate with ground stations on Earth and solving a major design challenge for any small spacecraft.

Finally, we have shown that the standard spacecraft subsystems (payload, ADCS, comms, power, thermal, and structures) for this mission appear viable, with their respective budgets closing with adequate margins, confirming the potential feasibility of the mission architecture.

4.2 Future Steps

Further work still needs to be done to continue developing this mission concept. Possible avenues of work for the CubeSats include computer-aided thermal analysis, more detailed CAD drawings including those showing the internal layout of the CubeSats, a dedicated command and data handling (CnDH) analysis rather than a partial analysis in the power and communications sections, and vibration and bending mode analysis, especially for any CubeSat group that uses a boom, such as the magnetometer group.

There is also work still to be done on the carrier spacecraft. Some examples include similar computer-aided thermal analysis, detailed CAD drawings of the exterior and

interior, CnDH analysis, and vibration analysis to those of the CubeSats. Standalone work also includes a sourced component list to complete a mass and volume budget for the structural analysis, a more detailed power subsystem analysis, and the design and modeling of a deployment system. Finally, the mission design as a whole could be improved by implementing a self-updating database so that the effects of changes to the mission design automatically propagate through all technical budgets rather than requiring manual updating. Such a database would significantly increase design iteration speed.

Bibliography

[1] SpaceX falcon heavy. https://www.spacex.com/vehicles/falcon-heavy/. [Accessed 13-04-2024].

[2] Spacex starship. https://www.spacex.com/vehicles/starship/. [Accessed 13-04-2024].

[3] Spire - Earth Online — earth.esa.int. https://earth.esa.int/eogateway/missions/spire. [Accessed 11-04-2024].

[4] AAC Clyde Space. Three axis satellite magnetometer.

[5] R. Abelson, Tibor Balint, H. Noravian, J. Randolph, Satter CM, G. Schmidt, and James Shirley. Enabling solar system exploration with small radioisotope power systems. *AGU Fall Meeting Abstracts*, 12 2005.

[6] R. Abelson, T.S. BALINT, K. Coste, J.O. Elliott, J.E. Randolph, G.R. Schmidt, T. Schriener, J.H. Shirley, and T.R. Spilker. Expanding frontiers with standard radioisotope power systems. Technical report, National Aeronautical and Space Administration, 2004.

[7] Caleb Adams. *High Performance Computation with Small Satellites and Small Satellite Swarms for 3D Reconstruction*. PhD thesis, 05 2020.

[8] APL. New horizons: The path to pluto and beyond.

[9] Australian Space Academy. Space communication calculations, 2023.

[10] Manlio Bacco, Pietro Cassarà, Marco Colucci, Alberto Gotta, Mario Marchese, and Fabio Patrone. A survey on network architectures and applications for nanosat and uav swarms. In Prashant Pillai, Kandeepan Sithamparanathan, Giovanni Giambene, Miguel Ángel Vázquez, and Paul Daniel Mitchell, editors, *Wireless and Satellite Systems*, pages 75–85, Cham, 2018. Springer International Publishing.

[11] Dylan Barnes, Andrew Cummings, and Paula do Vale Pereira. COMMUTE: Cubesat swarm orbital maneuvers for a mission to study uranus' atmospheric environment. In *Proceedings of the Small Satellite Conference, Weekend Poster Session 2, SSC23-WP2-38*, 2023.

[12] Linda Billings. *50 years of solar system exploration: Historical perspectives*. National Aeronautics and Space Administration, Office of Communications, NASA History Division, 2021.

[13] Robert E. Bitten, Stephen A. Shinn, and Debra L. Emmons. Challenges and potential solutions to develop and fund nasa flagship missions. *2019 IEEE Aerospace Conference*, Mar 2019.

[14] William J. Blackwell, Laura J. Bickmeier, R. Vincent Leslie, Michael L. Pieper, Jenna E. Samra, Chinnawat Surussavadee, and Carolyn A. Upham. Hyperspectral microwave atmospheric sounding. *IEEE Transactions on Geoscience and Remote Sensing*, 49(1):128–142, 2011.

[15] Scott J. Bolton, Richard M. Thorne, Sebastien Bourdarie, Imke de Pater, and Barry Mauk. Jupiter's inner radiation belts. In Fran Bagenal, Timothy E. Dowling, and William B. McKinnon, editors, *Jupiter. The Planet, Satellites and Magnetosphere*, volume 1, pages 671–688. 2004.

[16] Bilal MM Bomani. Cubesat technology past and present: Current state-of-the-art survey. Technical report, 2021.

[17] Scott Braun, Christopher Velden, Tom Greenwald, Derrick Herndon, Ralf Bennartz, Mark Demaria, Galina Chirokova, Robert Atlas, Jason Dunion, Frank Marks, Robert Rogers, Hui Christophersen, Bachir Annane, Bradley Zavodsky, and William Blackwell. Overview of the nasa tropics cubesat constellation mission. page 7, 09 2018.

[18] J. L. Burch, T. E. Moore, R. B. Torbert, and B. L. Giles. Magnetospheric Multiscale Overview and Science Objectives. , 199(1-4):5–21, March 2016.

[19] Craig Burkhard and Sasha Weston. The evolution of cubesat spacecraft platforms. In *AVT-336 Specialist'Meeting*, 2021.

[20] Stephen B. Cenko, Eric Christopher Bellm, Avishay Gal-Yam, Suvi Gezari, Varoujan Gorjian, April Jewell, Jeffrey W. Kruk, Shrinivas R. Kulkarni, Richard Mushotzky, Shouleh Nikzad, Anthony Piro, Eli Waxman, and Eran Oded Ofek. CUTIE: Cubesat Ultraviolet Transient Imaging Experiment. In *American Astronomical Society Meeting Abstracts #229*, volume 229 of *American Astronomical Society Meeting Abstracts*, page 328.04, January 2017.

[21] Soon-Jo Chung, Saptarshi Bandyopadhyay, Rebecca Foust, Giri P. Subramanian, and Fred Y. Hadaegh. Review of formation flying and constellation missions using nanosatellites. *Journal of Spacecraft and Rockets*, 53, 2016.

[22] CubeSpace Satellite Systems. Cubewheel gen 1.

[23] Howard D. Curtis. *Orbital Mechanics for Engineering Students*. Butterworth-Heinemann, 2020.

[24] E. Dotto, V. Della Corte, M. Amoroso, I. Bertini, J.R. Brucato, A. Capannolo, B. Cotugno, G. Cremonese, V. Di Tana, I. Gai, S. Ieva, G. Impresario, S.L. Ivanovski, M. Lavagna, A. Lucchetti, E. Mazzotta Epifani, A. Meneghin, F. Miglioretti, D. Modenini, M. Pajola, P. Palumbo, D. Perna, S. Pirrotta, G. Poggiali, A. Rossi, E. Simioni, S. Simonetti, P. Tortora, M. Zannoni, G. Zanotti, A. Zinzi, A.F. Cheng, A.S. Rivkin, E.Y. Adams, E.L. Reynolds, and K. Fretz. Liciacube - the light italian cubesat for imaging of asteroids in support of the nasa dart mission towards asteroid (65803) didymos. *Planetary and Space Science*, 199:105185, 2021.

[25] Dragonfly Aerospace. Mantis imager.

[26] C. P. Escoubet, A. Masson, H. Laakso, M. L. Goldstein, T. Dimbylow, Y. V. Bogdanova, M. Hapgood, B. Sousa, D. Sieg, and M. G. G. T. Taylor. Cluster after 20 years of operations: Science highlights and technical challenges. *Journal of Geophysical Research: Space Physics*, 126(8):e2021JA029474, 2021. e2021JA029474 2021JA029474.

[27] Chad Fish, Charles Swenson, Tim Neilsen, Bryan Bingham, Jake Gunther, Erik Stromberg, Steven Burr, Robert Burt, Mitch Whitely, Geoff Crowley, Irfan Azeem, Marcin Pilinski, Aroh Barjatya, and Justin Petersen. DICE mission design, development, and implementation: Success and challenges. *26th Small Satellite Conference Proceedings*, 2012.

[28] Joseph W. Gangestad, Brian S. Hardy, and David A. Hinkley. Operations, orbit determination, and formation control of the AeroCube-4 CubeSats. *27th Small Satellite Conference Proceedings*, 2013.

[29] Thomas Gardner, Brad Cheetham, Alec Forsman, Cameron Meek, Ethan Kayser, Jeff Parker, Michael Thompson, Tristan Latche, Rebecca Rogers, Brennan Bryant, and Tomas Svitek. CAPSTONE: A CubeSat pathfinder for the lunar gateway ecosystem. *35th Small Satellite Conference Proceedings*, 2021.

[30] James L. Green, Doug Cooke, Arthur W. Beckman, and Kristine M. Ramos. *Scientific Discovery and Societal Benefits with SLS Unique Launch Capability.*

[31] Yanping Guo and Robert W. Farquhar. New horizons mission design. *Space Science Reviews*, 140:49–74, 2008.

[32] Richard E. Hodges, Nacer E. Chahat, Daniel J. Hoppe, and Joseph D. Vacchione. The mars cube one deployable high gain antenna. In *2016 IEEE International Symposium on Antennas and Propagation (APSURSI)*, pages 1533–1534, 2016.

[33] Mark D Hofstadter and Bryan J Butler. Seasonal change in the deep atmosphere of uranus. *Icarus*, 165(1):168–180, 2003.

[34] Johns Hopkins University Applied Physics Lab. Space communication calculations.

[35] NASA JPL. Uranus.

[36] Zhigui Kang, Byron Tapley, Srinivas Bettadpur, John Ries, Peter Nagel, and Rick Pastor. Precise orbit determination for the GRACE mission using only GPS data. *Journal of Geodesy*, 80:322–331, 2006.

[37] Michael Krause, Ava Thrasher, Priyal Soni, Liam Smego, Reuben Isaac, Jennifer Nolan, Micah Pledger, E. Glenn Lightsey, W. Jud Ready, and John Christian. Lonestar: The lunar flashlight optical navigation experiment, 2024.

[38] NASA/Caltech Jet Propulsion Laboratory. Deep space network services catalog. *NASA/Caltech Jet Propulsion Laboratory*, 2015.

[39] NASA/Caltech Jet Propulsion Laboratory. Horizons system, 2023.

[40] W. Lan, R. Munakata, R. Nugent, and D. Pignatelli. Poly picosatellite orbital deployer mk. iii rev. e user guide, March 2014.

[41] E. R. Lancaster and R. C. Blanchard. Technical note d-5368: A unified form of lambert's theorem. Technical report, NASA, 1969.

[42] G. F. Lindal, J. R. Lyons, D. N. Sweetnam, V. R. Eshleman, D. P. Hinson, and G. L. Tyler. The atmosphere of uranus: Results of radio occultation measurements with voyager 2. *Journal of Geophysical Research: Space Physics*, 92(A13):14987–15001, 1987.

[43] Matthew Long, Allen Lorenz, Greg Rodgers, Eric Tapio, Glenn Tran, Keoki Jackson, Robert Twiggs, Thomas Bleier, and Stellar Solutions. A cubesat derived design for a unique academic research mission in earthquake signature detection. In *Proc. AIAA Small Satellite Conference*, 2002.

[44] A. Macario-Rojas, K.L. Smith, N.H. Crisp, and P.C.E. Roberts. Atmospheric interaction with nanosatellites from observed orbital decay. *Advances in Space Research*, 61(12):2972–2982, 2018.

[45] Christopher SR Matthes, David F Woerner, Terry J Hendricks, Jean-Pierre Fleurial, Knut I Oxnevad, Chadwick D Barklay, and June F Zakrajsek. Next-generation radioisotope thermoelectric generator study. In *2018 IEEE Aerospace Conference*, pages 1–9. IEEE, 2018.

[46] Moog, 2021.

[47] NASA. Mag technical write-up.

[48] NASA. Microlab 1.

[49] NASA. The nasa grace fact sheet.

[50] NASA. SpaceX Falcon 9 v1.2 Data Sheet. `https://sma.nasa.gov/LaunchVehicle/assets/spacex-falcon-9-v1.2-data-sheet.pdf`. [Accessed 13-04-2024].

[51] NASA. 2001 mars odyssey, 2003.

[52] NASA. Multi-mission radioisotope thermoelectric generator (mmrtg). *NASA*, 2020.

[53] NASA. Cassini mission, Jun 2021.

[54] NASA. Cassini spacecraft, Jun 2021.

[55] NASA. State-of-the-art of small spacecraft technology — avionics, May 2023.

[56] NASA. State-of-the-art of small spacecraft technology — communications, Nov 2023.

[57] NASA. State-of-the-art of small spacecraft technology — guidance, navigation, and control, May 2023.

[58] NASA. State-of-the-art of small spacecraft technology — thermal control, Nov 2023.

[59] National Academies of Sciences, Engineering, and Medicine. *Origins, Worlds, and Life: A Decadal Strategy for Planetary Science and Astrobiology 2023-2032*. The National Academies Press, Washington, DC, 2022.

[60] National Research Council. *Vision and Voyages for Planetary Science in the Decade 2013-2022*. The National Academies Press, Washington, DC, 2011.

[61] Cristóbal Nieto-Peroy and M. Reza Emami. Cubesat mission: From design to operation. *Applied Sciences*, 9(15), 2019.

[62] KARA Ozan. Future cubesat swarms pose significant communications challenges.

[63] Paradigma Technologies. K band transmitter.

[64] Nikolaos P. Paschalidis. Mass spectrometers for cubesats. 2nd Planetary CubeSat Science Symposium, 2017.

[65] Stephen Polly. Radioisotope thermoradiative cell power generator, Jul 2023.

[66] NASA Launch Services Program.

[67] Raj Thilak Rajan, Shoshana Ben-Maor, Shaziana Kaderali, Calum Turner, Mohammed Milhim, Catrina Melograna, Dawn Haken, Gary Paul, V Sreekumar, Johannes Weppler, et al. Applications and potentials of intelligent swarms for magnetospheric studies. *Acta Astronautica*, 193:554–571, 2022.

[68] Dennis C. Reuter, S. Alan Stern, John Scherrer, Donald E. Jennings, James W. Baer, John Hanley, Lisa Hardaway, Allen Lunsford, Stuart McMuldroch, Jeffrey Moore, Cathy Olkin, Robert Parizek, Harold Reitsma, Derek Sabatke, John Spencer, John Stone, Henry Throop, Jeffrey Van Cleve, Gerald E. Weigle, and Leslie A. Young. Ralph: A visible/infrared imager for the new horizons pluto/kuiper belt mission. *Space Science Reviews*, 140(1–4):129–154, June 2008.

[69] Nasir Saeed, Ahmed Elzanaty, Heba Almorad, Hayssam Dahrouj, Tareq Y Al-Naffouri, and Mohamed-Slim Alouini. Cubesat communications: Recent advances and future challenges. *IEEE Communications Surveys & Tutorials*, 22(3):1839–1862, 2020.

[70] Karan Sarda, Cordell Grant, Stuart Eagleson, Daniel Kekez, and Robert Zee. Canadian advanced nanospace experiment 2: on-orbit experiences with a three-kilogram satellite. 2008.

[71] Josh Schoolcraft, Andrew Klesh, and Thomas Werne. MarCO: Interplanetary mission development on a CubeSat scale. *Space Operations: Contributions from the Global Community*, 2017.

[72] R.C. Schulze and S. Hill. The new horizons high gain antenna: reflector design for a spin-stabilized bus at cryogenic temperatures. In *2004 IEEE Aerospace Conference Proceedings (IEEE Cat. No.04TH8720)*, volume 2, pages 966–974 Vol.2, 2004.

[73] Daniel Selva and David Krejci. A survey and assessment of the capabilities of cubesats for earth observation. *Acta Astronautica*, 74:50–68, 2012.

[74] Amy Simon, Francis Nimmo, and Richard C. Anderson. Uranus orbiter & probe. Technical report, NASA, 2021.

[75] David Alan Smith. Space launch system (sls) mission planner's guide. Technical report, 2018.

[76] Michael Swartwout. The first one hundred cubesats: A statistical look. *Journal of Small Satellites*, 2(2):213–233, Feb 2014.

[77] Jim Taylor. The deep space network: a functional description. *Deep Space Communications*, pages 15–35, 2016.

[78] Tempco. Kapton® heater wattage and watt density information.

[79] Paolo Tortora and Valerio Di Tana. LICIACube, the italian witness of DART impact on Didymos. *5th International Workshop on Metrology for AeroSpace Proceedings*, 2019.

[80] Tursdale Technical Services Ltd. The specification of hot wire anemometer manual pce-423.

[81] L. Wallace. The seasonal variation of the thermal structure of the atmosphere of uranus. *Icarus*, 54:110–132, 1983.

[82] Jianjian Wang, Chien-Hua Chen, Richard Bonner III, and William Anderson. Thermo-radiative cell - a new waste heat recovery technology for space power applications. In *AIAA Propulsion and Energy 2019 Forum*, 08 2019.

[83] J. W. Warwick, D. R. Evans, J. H. Romig, C. B. Sawyer, M. D. Desch, M. L. Kaiser, J. K. Alexander, T. D. Carr, D. H. Staelin, S. Gulkis, R. L. Poynter, M. Aubier, A. Boischot, Y. Leblanck, A. Lecacheux, B. M. Pedersen, and P. Zarka. Voyager 2 radio observations of uranus. *Science*, pages 102–106, 7 1986.

[84] James R. Wertz, David F. Everett, and Jeffery J. Puschell. *Space Mission Engineering: the New SMAD*. Microcosm Press, 2011.

[85] J. C. Zarnecki, M. Banaszkiewicz, M. Bannister, W. V. Boynton, P. Challenor, B. Clark, P. M. Daniell, J. Delderfield, M. A. English, M. Fulchingnoni, J. R. C. Garry, J. E. Geake, S. F. Green, B. Hathi, S. Jaroslawski, M. R. Leese, R. D. Lorenz, J. A. M. McDonnell, N. Merryweather-Clarke, C. S. Mill, R. J. Miller, G. Newton, D. J. Parker, P. Rabbetts, H. Svedhem, R. F. Turner, and M. J. Wright. The Huygens Surface Science Package. In A. Wilson, editor, *Huygens: Science, Payload and Mission*, volume 1177 of *ESA Special Publication*, page 177, January 1997.

Appendix A

Interplanetary Trajectory Code

A.1 Main

```
% day1 = datetime(2032,4,15)
% day2 = datetime(2034,12,31)
% time = caldays(between(day1,day2,'days'))

%Author: Dylan Barnes
%Last updated on 4/10/24

%Goal is to find the optimal transfer from Earth to Uranus with a flyby
%around Jupiter.

%Note. This code utilizes the coe_from_sv code originally distributed as
%part of Howard D. Curtis' Orbital Mechanics for Engineering Students, 4th
%edition.
```

```
% clc;
clear;

%% Data input

plotTraj = true;

dateResolution = 1; %How many days between iterations

%% FALCON HEAVY

% earthRangeStart = datetime(2032,2,15);
% earthRangeEnd = datetime(2032,6,15);

% earthRangeStart = datetime(2028,3,16); %optimal dry mass at for a 2028
    launch is 836kg with a launch on
% earthRangeEnd = datetime(2028,3,24); %3/21/28, flyby on 6/7/35, capture
    7/23/2039. tmEJ -1, res1

% earthRangeStart = datetime(2029,3,16); %optimal dry mass at for a 2029
    launch is 865kg with a launch on
% earthRangeEnd = datetime(2029,3,24); %3/20/29, flyby on 5/4/35, capture
    7/6/2039. tmEJ -1, res1

% earthRangeStart = datetime(2030,3,27); %optimal dry mass at for a 2030
    launch is 820kg with a launch on
```

```
% earthRangeEnd = datetime(2030,4,2); %3/30/30, flyby on 7/7/35, capture
    8/7/2039. tmEJ -1, res1

% earthRangeStart = datetime(2031,4,1); %optimal dry mass at for a 2031
    launch is 683kg with a launch on
% earthRangeEnd = datetime(2031,4,11); %4/5/31, flyby on 7/28/35, capture
    8/17/2039. tmEJ -1, res1

% earthRangeStart = datetime(2032,3,22); %optimal dry mass at for a 2032
    launch is 448kg with a launch on
% earthRangeEnd = datetime(2032,4,2); %3/8/32, flyby on 10/31/33, capture
    8/31/2038. tmEJ1, res1

% earthRangeStart = datetime(2032,4,10); %optimal dry mass at for a 2032
    launch is 478kg with a launch on
% earthRangeEnd = datetime(2032,4,20); %4/16/32, flyby on 10/14/35, capture
    9/24/2039. tmEJ -1, res1

% earthRangeStart = datetime(2033,5,1); %optimal dry mass at for a 2033
    launch is 790kg with a launch on
% earthRangeEnd = datetime(2033,5,9); %5/4/33, flyby on 11/24/34, capture
    4/14/2039. tmEJ1, res1

% earthRangeStart = datetime(2033,4,29); %optimal dry mass at for a 2033
    launch is 233kg with a launch on
% earthRangeEnd = datetime(2033,5,6); %5/4/33, flyby on 2/29/36, capture
    12/3/2039. tmEJ -1, res1
```

```
% earthRangeStart = datetime(2034,6,9); %optimal dry mass at for a 2034
    launch is 602kg with a launch on
% earthRangeEnd = datetime(2034,6,15); %6/12/34, flyby on 12/11/35, capture
    10/23/2039. tmEJ1, res1

% earthRangeStart = datetime(2034,5,30); %optimal dry mass at for a 2034
    launch is 73kg with a launch on
% earthRangeEnd = datetime(2034,6,6); %6/3/34, flyby on 11/24/36, capture
    5/7/2040. tmEJ -1, res1

%% SLS BLOCK 2

% earthRangeStart = datetime(2032,2,15);
% earthRangeEnd = datetime(2032,6,15);

% earthRangeStart = datetime(2028,3,17); %optimal dry mass at for a 2028
    launch is 3806kg with a launch on
% earthRangeEnd = datetime(2028,3,23); %3/22/28, flyby on 6/21/35, capture
    7/30/2039. tmEJ -1, res1

% earthRangeStart = datetime(2029,3,16); %optimal dry mass at for a 2029
    launch is 3466kg with a launch on
% earthRangeEnd = datetime(2029,3,24); %3/22/29, flyby on 5/24/35, capture
    7/16/2039. tmEJ -1, res1
```

```
% earthRangeStart = datetime(2030,3,27); %optimal dry mass at for a 2030
    launch is 3043kg with a launch on
% earthRangeEnd = datetime(2030,4,2); %3/30/30, flyby on 7/12/35, capture
    8/9/2039. tmEJ -1, res1

% earthRangeStart = datetime(2031,2,20); %optimal dry mass at for a 2031
    launch is 917kg with a launch on
% earthRangeEnd = datetime(2031,2,26); %2/23/31, flyby on 8/11/32, capture
    9/29/2037. tmEJ 1, res1

% earthRangeStart = datetime(2031,4,2); %optimal dry mass at for a 2031
    launch is 2389kg with a launch on
% earthRangeEnd = datetime(2031,4,8); %4/5/31, flyby on 7/28/35, capture
    8/17/2039. tmEJ -1, res1

% earthRangeStart = datetime(2032,3,26); %optimal dry mass at for a 2032
    launch is 1798kg with a launch on
% earthRangeEnd = datetime(2032,4,2); %3/30/32, flyby on 9/3/33, capture
    7/23/2038. tmEJ1, res1

% earthRangeStart = datetime(2032,4,10); %optimal dry mass at for a 2032
    launch is 1630kg with a launch on
% earthRangeEnd = datetime(2032,4,20); %4/15/32, flyby on 10/2/35, capture
    9/18/2039. tmEJ -1, res1

earthRangeStart = datetime(2033,5,1); %optimal dry mass at for a 2033
    launch is 3344kg with a launch on
```

```
earthRangeEnd = datetime(2033,5,9); %5/5/33, flyby on 10/1/34, capture
    3/18/2039. tmEJ1, res1

% earthRangeStart = datetime(2033,4,28); %optimal dry mass at for a 2033
    launch is 844kg with a launch on
% earthRangeEnd = datetime(2033,5,4); %5/1/33, flyby on 1/25/36, capture
    11/15/2039. tmEJ -1, res1

% earthRangeStart = datetime(2034,6,11); %optimal dry mass at for a 2034
    launch is 2957kg with a launch on
% earthRangeEnd = datetime(2034,6,17); %6/14/34, flyby on 10/24/35, capture
    9/29/2039. tmEJ1, res1

% earthRangeStart = datetime(2034,5,30); %optimal dry mass at for a 2034
    launch is 73kg with a launch on
% earthRangeEnd = datetime(2034,6,6); %6/3/34, flyby on 11/24/36, capture
    5/7/2040. tmEJ -1, res1

earthRange = earthRangeStart:dateResolution:earthRangeEnd;
% earthRange = datetime(2032,3,31);
% muEarth =
% tmEarth = 1;

%NOTE: Hohmann from Earth to Jupiter has a C3 of ~77 and takes 32.745
%months (996.6787 days)

%% FALCON HEAVY
```

```
% jupiterRangeStart = datetime(2034,1,1); %optimal C3 at 1/1/34 = 84.6, res
    is 5, tmJ is 1
% jupiterRangeEnd = datetime(2035,6,30);

% jupiterRangeStart = datetime(2035,5,25); %2028, tmEJ -1
% jupiterRangeEnd = datetime(2035,6,25);

% jupiterRangeStart = datetime(2035,4,15); %2029, tmEJ -1
% jupiterRangeEnd = datetime(2035,5,15);

% jupiterRangeStart = datetime(2035,6,21); %2030, tmEJ -1
% jupiterRangeEnd = datetime(2035,7,21);

% jupiterRangeStart = datetime(2035,7,15); %2031, tmEJ -1
% jupiterRangeEnd = datetime(2035,8,15);

% jupiterRangeStart = datetime(2033,10,12); %2032, tmEJ1
% jupiterRangeEnd = datetime(2033,11,12);

% jupiterRangeStart = datetime(2035,10,1); %2032, tmEJ -1
% jupiterRangeEnd = datetime(2035,10,31);

% jupiterRangeStart = datetime(2034,11,5); %2033, tmEJ1
% jupiterRangeEnd = datetime(2034,12,5);

% jupiterRangeStart = datetime(2036,2,15); %2033, tmEJ -1
```

```
% jupiterRangeEnd = datetime(2036,3,15);

% jupiterRangeStart = datetime(2035,12,5); %2034, tmEJ1
% jupiterRangeEnd = datetime(2036,1,5);

% jupiterRangeStart = datetime(2036,11,15); %2034, tmEJ -1
% jupiterRangeEnd = datetime(2036,12,15);

% jupiterRangeStart = datetime(2033,10,22); %optimal C3 at = , tmJ is 1
% jupiterRangeEnd = datetime(2033,11,8);
% jupiterRangeStart = datetime(2035,4,14); %optimal C3 at = , tmJ is 1
% jupiterRangeEnd = datetime(2035,4,16);
% jupiterRangeStart = datetime(2033,6,1); %optimal C3 at 10/29/34 is 89.9,
    res is 5, tmJ is 1
% jupiterRangeEnd = datetime(2034,6,1);

%% SLS BLOCK 2

% jupiterRangeStart = datetime(2034,1,1); %optimal C3 at 1/1/34 = 84.6, res
    is 5, tmJ is 1
% jupiterRangeEnd = datetime(2035,6,30);

% jupiterRangeStart = datetime(2035,6,1); %2028, tmEJ -1
% jupiterRangeEnd = datetime(2035,7,1);

% jupiterRangeStart = datetime(2035,5,1); %2029, tmEJ -1
% jupiterRangeEnd = datetime(2035,6,1);
```

```
% jupiterRangeStart = datetime(2035,7,1); %2030, tmEJ -1
% jupiterRangeEnd = datetime(2035,8,1);

% jupiterRangeStart = datetime(2032,8,1); %2031, tmEJ 1
% jupiterRangeEnd = datetime(2032,9,1);

% jupiterRangeStart = datetime(2035,7,15); %2031, tmEJ -1
% jupiterRangeEnd = datetime(2035,8,15);

% jupiterRangeStart = datetime(2033,8,21); %2032, tmEJ1
% jupiterRangeEnd = datetime(2033,9,21);

% jupiterRangeStart = datetime(2035,9,15); %2032, tmEJ -1
% jupiterRangeEnd = datetime(2035,10,15);

jupiterRangeStart = datetime(2034,9,15); %2033, tmEJ1
jupiterRangeEnd = datetime(2034,10,15);

% jupiterRangeStart = datetime(2036,1,15); %2033, tmEJ -1
% jupiterRangeEnd = datetime(2036,2,15);

% jupiterRangeStart = datetime(2035,10,5); %2034, tmEJ1
% jupiterRangeEnd = datetime(2035,11,5);

% jupiterRangeStart = datetime(2036,11,15); %2034, tmEJ -1
% jupiterRangeEnd = datetime(2036,12,15);
```

```
jupiterRange = jupiterRangeStart:dateResolution:jupiterRangeEnd;
% jupiterRange = datetime(2034,3,22);
muJupiter = 126686000;
tmJupiter = 1;

%% FALCON HEAVY

% uranusRangeStart = datetime(2035,6,30);
% uranusRangeEnd = datetime(2038,7,4);

% uranusRangeStart = datetime(2039,7,1); %2028, tmEJ -1
% uranusRangeEnd = datetime(2039,8,1);

% uranusRangeStart = datetime(2039,6,21); %2029, tmEJ -1
% uranusRangeEnd = datetime(2039,7,21);

% uranusRangeStart = datetime(2039,7,21); %2030, tmEJ -1
% uranusRangeEnd = datetime(2039,8,21);

% uranusRangeStart = datetime(2039,8,1); %2031, tmEJ -1
% uranusRangeEnd = datetime(2039,9,1);

% uranusRangeStart = datetime(2038,8,30); %2032, tmEJ1
% uranusRangeEnd = datetime(2038,9,20);

% uranusRangeStart = datetime(2039,9,10); %2032, tmEJ -1
```

```
% uranusRangeEnd = datetime(2039,10,10);

% uranusRangeStart = datetime(2039,4,10); %2033, tmEJ1
% uranusRangeEnd = datetime(2039,5,10);

% uranusRangeStart = datetime(2039,11,20); %2033, tmEJ -1
% uranusRangeEnd = datetime(2039,12,20);

% uranusRangeStart = datetime(2039,10,11); %2034, tmEJ1
% uranusRangeEnd = datetime(2039,11,11);

% uranusRangeStart = datetime(2040,5,1); %2034, tmEJ -1
% uranusRangeEnd = datetime(2040,5,31);

%% SLS BLOCK 2

% uranusRangeStart = datetime(2035,6,30);
% uranusRangeEnd = datetime(2038,7,4);

% uranusRangeStart = datetime(2039,7,11); %2028, tmEJ -1
% uranusRangeEnd = datetime(2039,8,11);

% uranusRangeStart = datetime(2039,7,1); %2029, tmEJ -1
% uranusRangeEnd = datetime(2039,8,1);

% uranusRangeStart = datetime(2039,7,21); %2030, tmEJ -1
% uranusRangeEnd = datetime(2039,8,21);
```

```
% uranusRangeStart = datetime(2037,9,15); %2031, tmEJ 1
% uranusRangeEnd = datetime(2037,10,15);

% uranusRangeStart = datetime(2039,8,1); %2031, tmEJ -1
% uranusRangeEnd = datetime(2039,9,1);

% uranusRangeStart = datetime(2038,7,10); %2032, tmEJ1
% uranusRangeEnd = datetime(2038,8,10);

% uranusRangeStart = datetime(2039,9,10); %2032, tmEJ -1
% uranusRangeEnd = datetime(2039,10,10);

uranusRangeStart = datetime(2039,3,5); %2033, tmEJ1
uranusRangeEnd = datetime(2039,4,5);

% uranusRangeStart = datetime(2039,11,1); %2033, tmEJ -1
% uranusRangeEnd = datetime(2039,12,1);

% uranusRangeStart = datetime(2039,9,16); %2034, tmEJ1
% uranusRangeEnd = datetime(2039,10,16);

% uranusRangeStart = datetime(2040,5,1); %2034, tmEJ -1
% uranusRangeEnd = datetime(2040,5,31);

uranusRange = uranusRangeStart:dateResolution:uranusRangeEnd;
% uranusRange = datetime(2039,5,4);
```

```
muUranus = 5794000;
tmUranus = 1;

%% Data input cont.

muSun = 132712440018;

earthEphem =
    table2timetable(readtable('EarthEphemeris_1_1_28-12_31_38.xlsx'));
jupiterEphem =
    table2timetable(readtable('JupiterEphemeris_12_31_32-12_31_45.xlsx'));
uranusEphem =
    table2timetable(readtable('UranusEphemeris_12_31_34-12_31_45.xlsx'));

if height(earthEphem)==0
    print('Error in collecting EarthEphem data')
end
if height(jupiterEphem)==0
    print('Error in collecting jupiterEphem data')
end
if height(uranusEphem)==0
    print('Error in collecting uranusEphem data')
end

% record = 0;

eitrcount = 0;
```

```
optimalLaunch = datetime(2032,3,15);
optimalFlyby = datetime(2034,11,31);
optimalCapture = datetime(2039,6,4);
optimalDryMass = -6000;
record=[0,0,0,0];

for earthItr = earthRange
%     Tau_TEarth = caldays(between(earthRangeStart,earthItr,'days'));
    eitrcount = eitrcount+1
    %Don't need anything here
    jitrcount = 0;
    for jupiterItr = jupiterRange
        jitrcount = jitrcount +1;
        Tau_TEJ = caldays(between(earthItr,jupiterItr,'days'));

        %Need first lambert here. DV1EJ gives the needed C3. DV2EJ is related
        %to the jupiter flyby

        %[VTransfer1, Vtransfer2, DeltaV1, DeltaV2] = LambertSolve(Tau_T,
            tm, mu, R1, V1, R2, V2)

        RE = table2array(earthEphem(earthItr,1:3));
        VE = table2array(earthEphem(earthItr,4:6));
        RJ = table2array(jupiterEphem(jupiterItr,1:3));
        VJ = table2array(jupiterEphem(jupiterItr,4:6));
```

```
        [V1EJ, V2EJ, DV1EJ, DV2EJ] = LambertSolve(Tau_TEJ, tmJupiter, muSun,
            RE, VE, RJ, VJ);



        uitrcount = 0;
        for uranusItr = uranusRange

            uitrcount=uitrcount+1;

            Tau_TJU = caldays(between(jupiterItr,uranusItr,'days'));

            %Need second lambert here. ?V1JU is related to the flyby. ?V2JU
                is related
            %to the slowdown burn.

            RU = table2array(uranusEphem(uranusItr,1:3));
            VU = table2array(uranusEphem(uranusItr,4:6));

            [V1JU, V2JU, DV1JU, DV2JU] = LambertSolve(Tau_TJU, tmUranus,
                muSun, RJ, VJ, RU, VU);

            %Need the flyby. Flyby needs V2EJ, V1JU, VJ, and muJ and gives
            %the boost ?V needed and the periapsis around jupiter.

%           [requiredDeltaV,r_peri] =
    FlybySolve(spacecraftHelioV1,spacecraftHelioV2,helioVPlanet,muPlanet)
```

```
[boostDeltaV,r_periBoost] = FlybySolve(V2EJ,V1JU,VJ,muJupiter);

%Need the final mass calculations. DV1EJ^2 gives the needed C3,
%which then gives wet mass using the equation from
    Mass_vs_C3.xlsx.

%           MassVC3 = @(x) -8090*log(x)+38153;
C3 = norm(DV1EJ)^2;
%           wetMass = -8090*log(C3)+38153;   %falcon heavy
wetMass = -19466*log(C3)+94100;   %SLS block 2

%We then subtract the fuel mass from the wet mass to get dry
%mass.

%% DeltaV to get into a capture orbit given rp and e - iffy!!
    Needs to be checked -> checked. All good
% radUran = 25362;      %km, volumetric mean radius
% radUran = 24973;      %km, polar radius 1 bar
radUran = 25559;      %km, equatorial radius 1 bar

eCap = .80;
altUranPeri = 4000;    %km
rPeriUran = radUran+altUranPeri;                %periapsis of
    capture orbit
rApoCap = (rPeriUran+(eCap*rPeriUran))/(1-eCap); %apoapsis of
    capture orbit
aCap = (rPeriUran+rApoCap)/2;
```

```
vPeriCap = sqrt(muUranus*((2/rPeriUran)-(1/aCap))); %using
    vis-viva to find v at periapsis
deltaVCap = abs(norm(DV2JU)-vPeriCap);   %finding the difference
    between v at periapsis and the uranocentric velocity of the
    spacecraft

%% Rocket equation to find fuel mass
deltaVFlyby = norm(boostDeltaV);
Isp = 348; %spacex merlin 1D Vacuum engine
g0 = 9.81/1000; %km/s^2
% wetOverDry = exp((deltaVFlyby+deltaVOpt)/(Isp*g0)) %using
    optimal capture
wetOverDry = exp((deltaVFlyby+deltaVCap)/(Isp*g0)); %doesn't
    take earth exit into account because that's entirely the
    falcon heavy.
dryMass = wetMass/wetOverDry;   %since wet mass is 3013kg, this
    is the correct dry mass, including the cubesats+fuel and the
    mothership
fuelMass = wetMass - dryMass;
% capFuel = 3013-3013/exp((deltaVCap)/(Isp*g0))
% flybyFuel = 3013-3013/exp((deltaVFlyby)/(Isp*g0))
capFuel = dryMass*exp(deltaVCap/(Isp*g0))-dryMass;
flybyFuel =
    (dryMass+capFuel)*exp(deltaVFlyby/(Isp*g0))-(dryMass+capFuel);
% test = dryMass*exp((deltaVFlyby+deltaVCap)/(Isp*g0))-dryMass
% test2 = capFuel+flybyFuel
```

```
%update recordkeeping

if dryMass > optimalDryMass
    optimalLaunch = earthItr;
    optimalTau_TEJ = Tau_TEJ;
    optimalTau_TJU = Tau_TJU;
    optimalFlyby = jupiterItr;
    optimalCapture = uranusItr;
    optimalDryMass = dryMass;
    optimalWetMass = wetMass;
    optimalC3 = C3;
    optimalFlybyDeltaVMag = deltaVFlyby;
    optimalFlybyDeltaV = boostDeltaV;
    optimalCaptureDeltaV = deltaVCap;
    optimalFlybyFuel = flybyFuel;
    optimalCaptureFuel = capFuel;
    optimalTotalFuelMass = fuelMass;
    optimalFlybyRadius = r_periBoost;
    optimalV1EJ = V1EJ;
    optimalV2EJ = V2EJ;
    optimalDV1EJ = DV1EJ;
    optimalDV2EJ = DV2EJ;
    optimalV1JU = V1JU;
    optimalV2JU = V2JU;
    optimalDV1JU = DV1JU;
    optimalDV2JU = DV2JU;
    optimalEarthSV = [RE,VE];
```

```
                optimalJupiterSV = [RJ,VJ];
                optimalUranusSV = [RU,VU];
            end
%             record(eitrcount,jitrcount,uitrcount)=norm(DV1EJ);
            record = [record;eitrcount, jitrcount, uitrcount, dryMass];
        end

    end
    jitrcount = 0;
end

% record(1)=[]
% C3 = min(record)^2;
% wetMass = -8090*log(C3)+38153
record(1,:)=[];

launchDates=record(:,1)*dateResolution+datenum(earthRangeStart)-1;
flybyDates=record(:,2)*dateResolution+datenum(jupiterRangeStart)-1;
captureDates=record(:,3)*dateResolution+datenum(uranusRangeStart)-1;

f1 = figure;
scatter3(launchDates,flybyDates,captureDates,40,record(:,4),'filled')
f1.Position = [440 376 708 421];

datetick('x',2)
datetick('y',2)
datetick('z',2)
```

```
title(sprintf('Launch Date, Jupiter Flyby Date, and Capture Date vs.
    Spacecraft Dry Mass (kg), tm = %d', tmJupiter));

xlabel('Launch Date')
ylabel('Flyby Date')
zlabel('Capture Date')
colormap jet
cb = colorbar;
cb.Label.String = 'Dry Mass (kg)';
view([-25.7703,31.8]);

%% Plotting Trajectory
if plotTraj == true
    added2pi=false;
    %plotting planets
    f2 = figure;
    scatter3(0,0,0,36,[0.9290 0.6940 0.1250],'filled');
    hold on;
    scatter3(optimalEarthSV(1),optimalEarthSV(2),optimalEarthSV(3),36,[0
        0.4470 0.7410],'filled');
    scatter3(optimalJupiterSV(1),optimalJupiterSV(2),optimalJupiterSV(3),36,[0.8500
        0.3250 0.0980],'filled');
    scatter3(optimalUranusSV(1),optimalUranusSV(2),optimalUranusSV(3),36,[0.3010
        0.7450 0.9330],'filled');
    %getting orbital elements from SV
    coeArc1Start=coe_from_sv(optimalEarthSV(1:3),optimalV1EJ,muSun);
```

```
coeArc1End=coe_from_sv(optimalJupiterSV(1:3),optimalV2EJ,muSun);
coeEarth=coe_from_sv(optimalEarthSV(1:3),optimalEarthSV(4:6),muSun);
coeJupiter=coe_from_sv(optimalJupiterSV(1:3),optimalJupiterSV(4:6),muSun);
%extracting arc 1 elements
aArc1 = coeArc1Start(7);
eArc1 = coeArc1Start(2);
OmegaArc1 = coeArc1Start(3);
iArc1 = coeArc1Start(4);
omegaArc1 = coeArc1Start(5);
%getting shape of 1st ellipse and transforming from polar to cartesian
theta = linspace(coeArc1Start(6),coeArc1End(6),360);
r=(aArc1.*(1-eArc1.^2))./(1+eArc1.*cos(theta));
x=r.*cos(theta);
y=r.*sin(theta);
z=zeros(size(x,2));
%    plot(x,y);
%creating a transformation matrix based on COEs to orient arc 1
%correctly and doing the multiplication
transformArc1 = [cos(omegaArc1),sin(omegaArc1),0;-
   sin(omegaArc1),cos(omegaArc1) ...
,0;0,0,1]*[1,0,0;0,cos(iArc1),sin(iArc1);0, ...
-sin(iArc1),cos(iArc1)]*[cos(OmegaArc1),sin(OmegaArc1) ...
,0;-sin(OmegaArc1),cos(OmegaArc1),0;0,0,1];
temp=zeros(3,3,size(x,2));
temp(1,1,:)=x;
temp(2,2,:)=y;
transformedArc1=zeros(3,3,size(x,2));
```

```
for i = 1:size(x,2);transformedArc1(:,:,i)=temp(:,:,i)*transformArc1;end
%recombining vectors and data processing.
newx=transformedArc1(1,1,:)+transformedArc1(2,1,:)+transformedArc1(3,1,:);
newy=transformedArc1(1,2,:)+transformedArc1(2,2,:)+transformedArc1(3,2,:);
newz=transformedArc1(1,3,:)+transformedArc1(2,3,:)+transformedArc1(3,3,:);
xArc1=newx(:);
yArc1=newy(:);
zArc1=newz(:);
plot3(xArc1,yArc1,zArc1);

%repeat for arc 2

coeArc2Start=coe_from_sv(optimalJupiterSV(1:3),optimalV1JU,muSun);
coeArc2End=coe_from_sv(optimalUranusSV(1:3),optimalV2JU,muSun);
coeUranus=coe_from_sv(optimalUranusSV(1:3),optimalUranusSV(4:6),muSun);
%extracting arc 2 elements
thetaArc2Start = coeArc2Start(6);
thetaArc2End = coeArc2End(6);
aArc2 = coeArc2Start(7);
eArc2 = coeArc2Start(2);
OmegaArc2 = coeArc2Start(3);
iArc2 = coeArc2Start(4);
omegaArc2 = coeArc2Start(5);
%getting shape of 2nd ellipse and transforming from polar to cartesian
if thetaArc2End<thetaArc2Start
    thetaArc2End=thetaArc2End+2*pi;
    added2pi=true;
```

```
    end
    theta = linspace(thetaArc2Start,thetaArc2End,360);
%     theta = linspace(0,2*pi,360);
    if added2pi
        for i=1:length(theta)
            if theta(i)>2*pi
                theta(i)=theta(i)-2*pi;
            end
        end
    end
    r=(aArc2.*(1-eArc2.^2))./(1+eArc2.*cos(theta));
    x=r.*cos(theta);
    y=r.*sin(theta);
    z=zeros(size(x,2));
%     plot(x,y);
    %creating a transformation matrix based on COEs to orient arc 2
    %correctly and doing the multiplication
    transformArc2 =
        [cos(omegaArc2),sin(omegaArc2),0;-sin(omegaArc2),cos(omegaArc2),0;0,0,1]*[1,0,0;0,cos
    temp=zeros(3,3,size(x,2));
    temp(1,1,:)=x;
    temp(2,2,:)=y;
    transformedArc2=zeros(3,3,size(x,2));
    for i = 1:size(x,2);transformedArc2(:,:,i)=temp(:,:,i)*transformArc2;end
    %recombining vectors and data processing.
    newx=transformedArc2(1,1,:)+transformedArc2(2,1,:)+transformedArc2(3,1,:);
    newy=transformedArc2(1,2,:)+transformedArc2(2,2,:)+transformedArc2(3,2,:);
```

```
    newz=transformedArc2(1,3,:)+transformedArc2(2,3,:)+transformedArc2(3,3,:);
    xArc2=newx(:);
    yArc2=newy(:);
    zArc2=newz(:);
    plot3(xArc2,yArc2,zArc2);

    xlabel('Distance in x (km)')
    ylabel('Distance in y (km)')
    zlabel('Distance in z (km)')
    title(sprintf('Earth-Jupiter-Uranus Transfer with Expanded Z Axis, tm =
        %d', tmJupiter));
    f2.Position = [380 88 989 709];
    view([51.8060,38.6439]);

    legend('ssb','Earth','Jupiter','Uranus','EJ Trajectory', 'JU
        Trajectory');
end
```

A.2 Lambert Problem Solver

```
    function [VTransfer1, Vtransfer2, DeltaV1, DeltaV2] =
        LambertSolve(Tau_T, tm, mu, R1, V1, R2, V2)
%LambertSolve Calculate a Lambert transfer between two points


%% Step 1: deltatheta and A
```

```
r1 = norm(R1);                          %km
r2 = norm(R2);                          %km
cosdeltatheta = dot(R1,R2)/(r1*r2);
A = tm*sqrt(r2*r1*(1+cosdeltatheta)); %km

%% Step 2: Universal vars

psii = 0;
C2i = 1/2;
C3i = 1/6;
psiupi = 4*pi^2;
psilowi = -4*pi;

%% Step 3: iterate
test = true;
iterationcounter = 1;
while test
    iterationcounter = iterationcounter+1;
    yi = r1+r2+(A*((psii*C3i)-1)/sqrt(C2i));
    chii = sqrt(yi/C2i);
    deltati = (((chii^3)*C3i)+(A*sqrt(yi)))/sqrt(mu);
    deltati_test = deltati/(60*60*24);

    if (abs(deltati_test - Tau_T)/Tau_T) < 1E-6
        test = false;
        break
```

```
    end

    if deltati_test <= Tau_T
        psilowi = psii;
    end
    if deltati_test > Tau_T
        psiupi = psii;
    end

    psii = (psiupi+psilowi)/2;

    if psii > 1E-6
        C2i = (1-cos(sqrt(psii)))/psii;
        C3i = (sqrt(psii)-sin(sqrt(psii)))/sqrt(psii^3);
    elseif psii < -1E-6
        C2i = (1-cosh(sqrt(-psii)))/psii;
        C3i = (sinh(sqrt(-psii))-sqrt(-psii))/sqrt(-psii^3);
    else
        C2i = 1/2;
        C3i = 1/6;
    end


end

%% Step 4: Find F, G, Gt
```

```
F = 1 - (yi/r1);

G = A*sqrt(yi/mu);    %sec

Gt = 1 - (yi/r2);


%% Step 5: find deltaVs


VTransfer1 = (R2 - (F*R1))/G;

Vtransfer2 = ((Gt*R2)-R1)/G;


DeltaV1 = VTransfer1-V1;

% MagDeltaV1 = norm(DeltaV1)


DeltaV2 = Vtransfer2-V2;

% MagDeltaV2 = norm(DeltaV2)

end
```

A.3 Planetary Flyby Solver

```
    function [requiredDeltaV,r_peri] =

        FlybySolve(spacecraftHelioV1,spacecraftHelioV2,helioVPlanet,muPlanet)

%UNTITLED4 Summary of this function goes here

%   Detailed explanation goes here


planetcentricV1 = spacecraftHelioV1-helioVPlanet; %km/s

planetcentricV2 = spacecraftHelioV2-helioVPlanet; %km/s
```

```
BetaAngle =
    acosd(dot(planetcentricV1,planetcentricV2)/(norm(planetcentricV1)*
                                                    norm(planetcentricV2)))/2;
                                                        %deg
turningAngle = 180-2*BetaAngle;      %deg

eHyperbola = 1/(sind(turningAngle/2));

vinf=norm(planetcentricV1);

r_peri = ((eHyperbola-1)*muPlanet)/vinf^2; %km
%Unsure if this is right, trying not to assume 2d
vinf2 = vinf*(planetcentricV2/norm(planetcentricV2));

heliov2scaled = vinf2+helioVPlanet;

requiredDeltaV = spacecraftHelioV2-heliov2scaled;

% requiredDeltaV = planetcentricV2-vinf2

requiredDeltaVNorm = norm(requiredDeltaV);
end
```